

# Vertical Profiling of Horizontal Currents Using Freely Sinking and Rising Probes

## Chapter Outline

<b>10.1. Importance of Vertical Profile Measurements of Ocean Currents</b>	297	10.2.7. Freely Falling, Acoustically Self-Positioning Driftsonde (White Horse) 320
<b>10.2. Technologies Used for Vertical Profile Measurement of Ocean Currents</b>	300	10.2.8. Freely Rising Acoustically Tracked Expendable Probes (Popups) 322
10.2.1. Freely Sinking and Wire-Guided Relative Velocity Probes	300	10.3. Technologies Used for Vertical Profile Measurements of Oceanic Current Shear and Fine Structure 325
10.2.2. Bottom-Mounted, Winch-Controlled Vertical Automatic Profiling Systems	302	10.3.1. Free-Fall Shear Profiler (Yvette) 326
10.2.3. Acoustically Tracked Freely Sinking Pingers	305	10.3.2. Acoustically Tracked Free-Fall Current Velocity and CTD Profiler (TOPS) 326
10.2.4. A Freely Sinking and Rising Relative Velocity Probe (Cyclesonde)	308	10.4. Technologies Used for Vertical Profile Measurements of Oceanic Current Shear and Microstructure 329
10.2.4.1. Operation	309	10.4.1. Towed Acoustic Transducer 329
10.2.4.2. Advantages	310	10.4.2. Free-Fall Probe (PROTAS) 330
10.2.5. A Freely Falling Electromagnetic Velocity Profiler	311	10.4.3. Free-Falling Lift-Force Sensitive Probes 332
10.2.6. Free-Falling, Acoustically Tracked Absolute Velocity Profiler (Pegasus)	318	10.5. Merits and Limitations of Freely Sinking/Rising Unguided Probes 335
		References 335
		Bibliography 337

## 10.1. IMPORTANCE OF VERTICAL PROFILE MEASUREMENTS OF OCEAN CURRENTS

Qualitatively, the ocean is regarded as a deck of cards (water layers) wherein each card moves horizontally at a given velocity. The difference in horizontal velocity of neighboring water layers in the ocean gives rise to what is known as *vertical shear of horizontal current velocity* (defined as the derivative of current with respect to depth). Although current shears are most frequently found in the upper layers of the water column, primarily because different time responses by water layers at different depths to a fluctuating wind regime induce high lateral shear, they are also found within the main thermocline and within 500 m of the seafloor.

By the early 1960s it had become increasingly evident that not only the surface waters of the oceans but also the deep waters are active over a wide range of frequencies

(e.g., Crease, 1962; Pochapsky, 1966). With the advent of continuously profiling seawater temperature and salinity systems, oceanographers became aware of a new world of fine and microstructure in the density field of the oceans. A wide spectrum of small-scale, predominantly stratified structure was found at all depths in tropical as well as polar oceans (Stommel and Federov, 1967; Neshyba et al., 1971). It could be inferred from basic physical considerations that this complex density field cannot exist without a corresponding richness in the velocity field. What was missing was the ability to resolve the fine-scale velocity simultaneously with the density field in order to explore and quantify the causal relationship between the two.

There has been evidence to suggest that kinetic energy propagates downward, perhaps as isolated events or packets of energy. Based on measurements from a few sites, Rossby and Sanford (1976) showed that the inertial frequency-band energy propagates downward at a group velocity with

a vertical component of about 0.5 mm/s. In general, current variability is observed throughout the water column. Depth dependence of water currents at different regions of the oceans is influenced by various factors, such as the presence of ridges, gorges, valleys, and banks. It was suspected that a current velocity field in the deep ocean along the Continental rise contains significant spatial gradients in the vertical. For instance, measurements of the vertical profile of currents carried out by Rossby (1969) on the southern slope of the Plantagenet Bank southwest of Bermuda showed that the Bank has a pronounced influence on the local flow. In this region, at depths less than 500 m, the currents are found to be swift at more than 30 cm/s, whereas at this depth a sudden transition to a slow drift of the deep water along the topography was observed. Changes in horizontal velocities with depth are not gradual but occur in regions of limited vertical extent where current velocity differences of 10–20 cm/s in 10 m were observed. The effective blocking of the deep water by the Bank causes a local depression of the main thermocline deeper than is typical for the Bermuda area. Influence of ridge valleys on the structure and evolution of vertical profiles of horizontal motions is particularly interesting. Garcia-Berdeal et al. (2006) reported fascinating vertical structures of time-dependent water currents in the axial valley at the Endeavor Segment of the Juan de Fuca Ridge.

Oceanic water current velocity shear has great importance in turbulent mixing and dispersal effects. An interesting application of vertical profile measurements in oceanography is in the study of fine structures and microstructures and velocity shear in the water column. Ocean-current velocity profile observations have revealed considerable complexity to the vertical structure or distribution of currents in the deep sea. An individual vertical profile is composed of a superposition of a wide spectrum of different spatial and temporal scales of motions operating simultaneously. In a study of low-frequency variability of the velocity profile at one site, Rossby (1974) found that monthly or even weekly sampling was inadequate to follow the time evolution of the velocity profile. Low-frequency (quasi-geostrophic) structures can be advected past the observation site in a matter of days. Moreover, high-frequency contributions, such as those due to internal tidal or inertial period motions, are important constituents to an individual profile. Thus, repeated current-velocity profiles at one site are needed in order to estimate the energy contributed by a variety of time-dependent motions.

General knowledge of oceanic motions has increased considerably during the past decades, primarily due to the successful use of moored current meters. The technology of mooring and maintaining chains of current meters in the deep ocean has steadily improved; moorings became maintainable for even a year or more, yielding time series long enough to cover the greater part of the spectrum of oceanic motions. Observation of poor vertical coherence at

inertial frequency for current meters separated 100 m in the vertical, based on examination of an extensive data bank at the Woods Hole Oceanographic Institution (Perkins, 1970), gave rise to the conjecture that some of the most energetic temporal frequencies are badly sampled (aliased) in the vertical by typical fixed instrument spacing.

Considering further what is already known about temperature and salinity distributions in the oceans—to cite an example, data from the San Diego Trough showed conductivity structures with vertical wavelengths down to less than a centimeter (Gregg and Cox, 1971)—it is amply clear that vertical profiles of scalar or vectoral quantities of interest cannot be obtained with an economical number of fixed instruments. The often observed extremely low correlation between motions at different depth levels (Webster, 1968, 1969), together with the great expense of current meter chains, indicated the necessity for additional tools (say, vertically moving sensor packages providing high-resolution profiles) to measure ocean currents effectively over a variety of space and time scales. Obviously, it would be interesting to explore how these horizontal motions on different time scales couple in the vertical. This calls for fine-resolution measurements of horizontal motions over both small and large vertical separations. Besides being suitable for directly verifying coupled thermal and circulation models in the ocean and large lakes, the dataset obtained from vertical profilers possessing fine spatial and temporal resolution should provide an understanding of a number of geophysical phenomena and processes, such as the evolution of the surface mixed layer; the generation and decay of internal waves and seiches; and the turbulent transport and mixing of heat, momentum, and water masses.

With rapid improvements in oceanographic instruments in post World War period, large fluctuations in the vertical and horizontal distributions of seawater temperature and salinity were found. These fluctuations have come to be called *fine structure* or *microstructure*, depending on their wavelengths. Such fluctuations were expected to occur in the ocean currents as well, in which wavelengths  $\lambda$ , shorter than 1 m, came to be known as microstructure, and wavelengths in the range 1–100 m are known as fine structure.

The study of oceanic microstructure is really a study of oceanic turbulence and mixing. The source of the turbulent energy and the mechanisms of extracting the energy must be determined. It may then be possible to understand the effect of the turbulence on the temperature and salinity profiles. Observations and photographs by Woods and Fosberry (1967) in the thermocline off Malta indicated that shear instability is a source of turbulent energy. Gregg and Cox (1971) reported measurements of vertical profiles of temperature microstructure to the millimeter range in the ocean. Osborn (1969) noticed oceanic regions of intense gradient activity several meters thick, which are suggestive of the turbulent patches observed by Woods (1968) in the

thermocline. The local Richardson number ( $Ri$ ) is considered the most important parameter that controls the stability of a stratified fluid and thus occurs as the essential ingredient in a wide range of schemes for parameterizing the turbulent fluxes. A necessary criterion for the growth of infinitesimal shear instability is:

$$Ri = \frac{g \frac{\partial \rho}{\partial z}}{\rho} \left( \frac{\partial U}{\partial z} \right)^2 < \frac{1}{4} \quad (10.1)$$

To evaluate the Richardson number ( $Ri$ ), it is necessary to know the vertical component of the density gradient  $\left( \frac{\partial \rho}{\partial z} \right)$  and the vertical shear of the horizontal current velocity  $\left( \frac{\partial U}{\partial z} \right)$ . The vertical profile of the density can be calculated from vertical profiles of the temperature and electrical conductivity of the ambient ocean water (i.e., CTD measurements). Techniques for measuring these parameters are given in the literature (e.g., Osborn and Cox, 1972; Gregg and Cox, 1972). A quantitative study of the roles of shear instability in generating oceanic microstructure requires detailed vertical profiles of the shear of the horizontal velocity.

In isotropic turbulence, the energy dissipated by viscosity can be estimated from (Hinze, 1959):

$$\varepsilon = 7.5\nu \left( \frac{\partial u}{\partial z} \right)^2 \quad (10.2)$$

In this expression,  $\varepsilon$  is the viscous energy dissipation,  $\nu$  is the coefficient of kinematic viscosity, and  $u$  is one horizontal component of the velocity. There is evidence that turbulence in the ocean is not generally isotropic (Grant et al., 1968; Nasmyth, 1970) and much work needs to be done to determine the three-dimensional nature of oceanic turbulence. It may be argued that the vertical shears are a significant part of the energy dissipation, and if the turbulence is not isotropic, it will change the numerical coefficient from 7.5 (in Equation 10.2) to a lower value, which will still be greater than 2. The turbulence is more likely to be isotropic where  $\varepsilon$  is large, on the order of  $10^{-3}$  erg/cm<sup>3</sup>/s or more, in which case the rms shear is  $\sim 10^{-1}$ /s. When the energy dissipation is low, the isotropic formula probably overestimates the dissipation rate. It might, therefore, be appropriate to change the factor 7.5 (in Equation 10.2) to  $5 \pm 2.5$  (Osborn, 1974). There is an increasing belief that it is the catastrophic events and not the mean situations that are important in turbulent transfer in the ocean. Therefore, more interest lies in the regions with high values of  $\varepsilon$  rather than low values.

In the past, measurements of small-scale velocity structures in the ocean were attempted, in limited depths only, by the use of moored current meter chains. Maintaining such moorings at large depths in the open ocean is prohibitively expensive. Furthermore, in situations where

intense current are to be measured, it is difficult to maintain these moorings. Additionally, these current profiling installations using a series of Eulerian current meters fastened to a tether are not conveniently mobile, nor are the installations readily adaptable to changing situations. Ideally, a single package scanning the entire water column repeatedly to sense the vertical distribution of horizontal motions with high vertical resolution is the preferred choice.

Single-probe profiling techniques have emerged as an attractive alternative tool to effectively measure vertical profiles of horizontal currents over considerable vertical distances while retaining high resolution of the small-scale features without being contaminated by mooring-line motions. Ideally, one might want a single package scanning the entire water column in order to sense the vertical distribution of horizontal motions with high vertical resolution. This basic necessity resulted in the development of single-probe profiling techniques. In fact, awareness of many complex features of oceanic motions, such as sharp and discrete shear zones, internal waves, and eddies in the ocean, has been enhanced by current velocity profile observations.

Measurements of the vertical structure of ocean currents are important for a wide variety of studies and operational applications. These include estimating depth-dependent variability of inertial and near-inertial motions in a stratified rotating fluid under the influence of topographical constrictions (e.g., over ocean ridges and valleys); study of layered current structure (attributed to the mixing process); quantifying/examining the velocity structure in hydrothermal plumes within a few hundred meters of the bottom (Thomson et al., 1989); estimation of volume transport; understanding the stratification of current jets; and so forth.

Deep-water current-velocity profiles are essential for studying interesting phenomena such as inertial oscillations and equatorial currents. The 1950s and subsequent years witnessed a rapid evolution of new methods of measuring ocean currents. The generally most useful instrument remained the self-recording current meter, which is capable of operating unattended for long periods of time. These meters are commonly used on deep-sea moorings, usually with several Eulerian current meters located at different depths. Whereas this method provides excellent time coverage, the current-versus-depth information is obviously limited to the number of instruments that can be afforded.

Fundamental discoveries have been made with the first application of new profiling technologies. These include, for example, the ratio of upward to downward energy flux in inertial waves (Leaman and Sanford, 1975) and the stack of alternate eastward and westward currents on the equator below the thermocline, known as the *deep jets* (Luyten and Swallow, 1976). Current profiles in mid-ocean ridges and their valleys are particularly interesting. For example,

within the axial valley of the Endeavor Ridge (well known as a hydrothermal vent region), located off the coasts of Washington and Oregon, a significant part of hydrothermal fluid and heat is released in the form of low-temperature diffuse plumes that rise 10–50 m above the bottom (Trivett and Williams, 1994; Rona and Trivett, 1992) and therefore remain within the confines of its valley. The vertical structure of water flows within the valley has important implications for the transport of hydrothermal vent fluid and the dispersal of larvae of vent organisms (Mullineaux and France, 1995).

Clearly, free-fall profilers are useful in strong currents where current meter moorings cannot be applied. Other applications include the study of internal waves and local dynamic investigations of ocean fronts and processes that are intermittent with respect to depth, such as lateral intrusions of different water masses. Obviously, the wide variety of applications of vertical profile measurements of horizontal currents in the ocean attracted the design and development of a number of vertical profiling instruments over a period of time, based on different principles of operation. These tools are addressed in the following sections.

## 10.2. TECHNOLOGIES USED FOR VERTICAL PROFILE MEASUREMENT OF OCEAN CURRENTS

The traditional method of measuring vertical profiles of horizontal currents is to use conventional fixed-point current meter (CM) moorings. However, moorings with fine vertical resolution (of the order of a few cm or tens of cm required for understanding a number of geophysical phenomena) are impractical and uneconomical. Furthermore, measurements using CM moorings are usually limited to depths far below the sea surface because of the disturbing influence of waves on the subsurface float. To circumvent such difficulties associated with moored CM chain measurements, various ingenious technologies have been developed from time to time for vertical profile measurement of ocean currents using a single package of freely moving sensors or a fixed remote sensing probe.

Basically, two methods are employed in the single-probe current profiling scheme. One method employs free-falling, wire-guided, or free-falling/rising autonomous probes as a means for measuring the vertical profiles of horizontal currents in the ocean. Launched from a ship, the probe falls freely, with no connections to the sea surface. The probe, in some designs, is capable of penetrating deep into the water column. The other method is acoustic Doppler profiling to remotely measure velocity profiles.

The first method, the free-falling probe, utilizes two basic techniques to measure current profiles. In one

technique, a pinger is acoustically tracked while it sinks or rises, much as a weather balloon is tracked using electromagnetic signals and the pinger's trajectory is thus determined. In the other technique, the trajectory of the probe is determined without the use of acoustic tracking. In either case, vertical profiles of horizontal current velocities are estimated from the trajectory described by the freely moving probe. Before the advent of ADCPs, freely moving sensor packages were the only available tools for high-resolution measurement of vertical profiles of horizontal currents in the ocean. This chapter addresses technologies using such moving packages. (ADCPs are discussed in chapter 11.)

### 10.2.1. FREELY SINKING AND WIRE-GUIDED RELATIVE VELOCITY PROBES

Several attempts have been made in the past to measure vertical profiles of horizontal currents. One of the most successful techniques is the *free-drop* technique (Richardson and Schmitz, 1965; Richardson et al., 1969). This method is ideally suited for fast surveys over considerable horizontal distances, yielding the mass transport through a cross-section. Its vertical resolution, however, is limited. A very high resolution has been achieved by Plaisted and Richardson (1970), who used a small winch mounted on a drifting sparbuoy to lower two current meters, thus obtaining relative profiles. A disadvantage of this method was the need for a highly accurate navigation system in order to convert the measured current to absolute current.

Duing and Johnson (1972) reported a simple, relatively inexpensive method for repeated observations of high-resolution current profiles, in which a profiling current meter (PCM) is constrained to roll down an anchored taut wire, with the roller attachment providing the necessary decoupling of the instrument from vertical wire motions. In this method, current profile measurements are carried out from anchored vessels. Figure 10.1 shows the principle of the profiling method. The profiler consists of a self-contained Aanderaa CM attached to a cylindrical hull. The density of the instrument package is slightly greater than that of the surrounding water. The Savonius rotor extends out from the bottom side of the cylindrical hull when it is in its horizontal working position. The entire package is attached by a roller to a taut wire suspended beneath the anchored ship and allowed to descend slowly through the entire water column. During operations in the Florida Current, Duing and Johnson (1972) found that the descent rate of the instrument was most favorable when it had approximately 1,000 g mean negative buoyancy. The principle of the ballasting procedure Duing and Johnson adopted is the following: The effective density of the instrument package can be measured and adjusted to the desired range by submerging it in a saltwater tank at

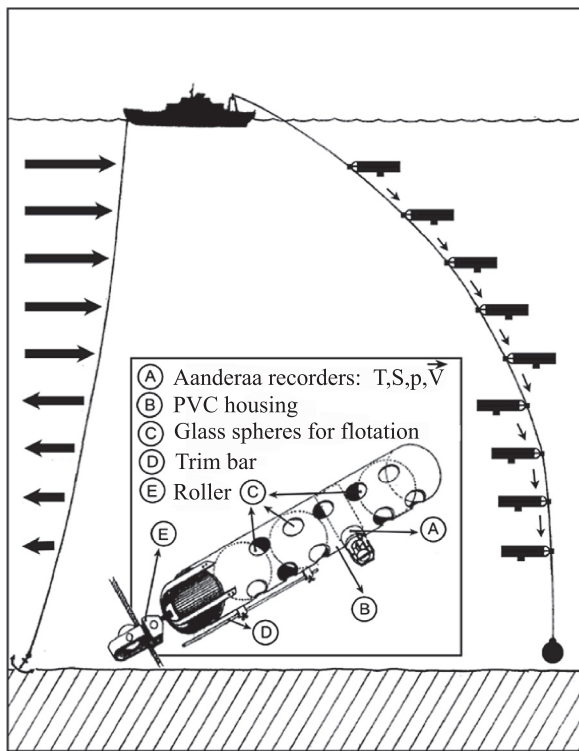


**FIGURE 10.1** Principle of the current-profiling method in which a profiling current meter (PCM) is constrained to roll down an anchored taut wire, with the roller attachment providing the necessary decoupling of the instrument from vertical wire motions. (Source: Duing and Johnson, 1972.)

a known salinity and temperature and by measuring its overweight with a scale (say, a spring balance) mounted above the tank. The adjustment is made with the use of the following formula (Duing and Johnson, 1972):

$$\rho = \rho_w + \frac{\Delta m_{ow}}{V} + \frac{\Delta m_a}{V} \quad (10.3)$$

In this expression,  $\rho$  is the desired effective density of the instrument;  $V$  is the volume of the instrument;  $\rho_w$  is the density of the tank water;  $\Delta m_{ow}$  is the measured overweight; and  $\Delta m_a$  is the mass added or subtracted. The mean buoyancy is  $(\bar{\rho} - \rho)g$ . In this,  $\bar{\rho}$  is the estimated mean density of the oceanic water column to be sampled. Ballast is added or subtracted by changing the amount of water in the forward and aft glass spheres inside the profiler hull. A certain amount of ballast is added near the instrument's center of buoyancy in the form of variously sized shackles to allow for ballast corrections on board ship.

Because the flow of water has to be perpendicular to the axis of the Savonius rotor, the profiler must be horizontally trimmed. This is done during the ballasting procedure by injecting water into the aft or forward glass spheres and by moving the additional shackles fore or aft. Once the instrument is horizontally trimmed, the center of buoyancy

of the profiler is determined by using a fulcrum to balance the instrument in water to a horizontal position. During operations at sea, it is thus possible to vary the sink rate of the instrument without changing the horizontal trim of the profiler by adding or removing weight from the center of buoyancy.

In operation, the PCM is attached to the taut wire above the sea surface by means of the roller and then lowered into the water and released by tripping a hook attached to its forward end. The hollow glass spheres inside the profiler hull provide an excellent acoustic target, and it is thus possible to follow the descent of the PCM on the ship's precision echo sounder. By this means, it is possible to monitor the sinking speed of the instrument on board ship and to change it, if necessary, by adding or subtracting weight from the center of buoyancy of the profiler hull.

Due to the catenary shape of the suspended wire and due to the vertically varying current profile, the sinking speed of the profiler varies with depth. Typical values are 15–20 cm/s in the upper 100 m and 5–8 cm/s in the deeper layers. A profile to 500 m is completed in approximately one hour. Because of high wire angles and larger currents in the upper layer, a horizontal motion of the profiler occurs that produces a velocity error, which needs to be corrected, as described later. The advantages of this method are the following (Duing and Johnson, 1972):

- A single instrument yields high-resolution vertical profiles.
- The axis of the Savonius rotor (i.e., a current-measuring sensor) remains always perpendicular to the flow of water, as expected, because of the horizontal trimming of the hull.
- The 2-meter-long profiler hull acts as a stable current vane.
- The roller attachment decouples the instrument from vertical wire motions.

If the profiler is deployed in a high-speed flow regime, there is an advantage of stabilization of the heading of the anchored ship. However, there are also some disadvantages. The greatest of these is the occurrence of large angles in the suspended wire along which the PCM descends. As a result of the wire angle, the PCM has a horizontal component to its motion as it descends; this component subtracts from the actual current speed. To correct for this, the product of the descent rate and the wire angle as a function of depth is calculated and added to the measured current. The wire shape as a function of depth is measured by taking the slant range to the PCM, measured by the sonar, together with its depth as measured by the PCM's pressure sensor. These two values in the  $x$ - $z$  plane provide a locus of points that is an image of the wire shape. To check this correction and to obtain rough information on the accuracy of an

instantaneous downward profile, the profiler may be stopped at discrete depth intervals while being raised. It must, however, be borne in mind that this check is only approximate, because the instrument hangs by its forward section at these stops and, consequently, is tilted. The tilt should be small in the high-intensity currents.

It is difficult to quantify the errors involved in the current profiles that have been measured by this technique. *In situ* comparison is one possible option. The individual sources of errors may be broken into two categories: those that are introduced by the profiling technique and those that are common with moored current meters. Accordingly, the following errors contribute to the total error crept into the measurements made by this method (Duing and Johnson, 1972):

- 1. Errors introduced by the profiling technique:**
  - Deviation of the profiler from its horizontal trim position
  - Induction of rotations or slowdown of the Savonius rotor due to vertical descent
  - Errors in determining the wire shape
  - Depth errors due to error of pressure sensor
- 2. Errors common with moored current meters:**
  - Inertia of the Savonius rotor in the presence of rapidly changing currents
  - Wire vibrations in intense currents
  - Horizontal motions of the supporting platform
  - Basic calibration errors

The effects of rotor inertia are greater in the profiling technique than in a moored current meter because the profiling meter is likely to pass through regions of large current shear. In addition, very little is known about wire vibrations in intense currents. Anchored ships in the deep ocean are known to exert swaying motions of the order of 15 cm/s. Figure 10.2 provides two selected profiles obtained using the PCM method from the same location in the Florida Straits in two different months in 1970. These two profiles of considerably different patterns from the same location emphasize the importance of the time-dependent aspect of current profiles in the Florida Straits.

### 10.2.2. Bottom-Mounted, Winch-Controlled Vertical Automatic Profiling Systems

The Vertical Automatic Profiling System (VAPS) is a profiling device specifically designed for vertical profile measurements in low-current regimes (e.g., typical of deep lakes). However, it can be deployed in coastal waters as well if the horizontal currents are not too large. Ward-Whate (1977) described a device that is designed to

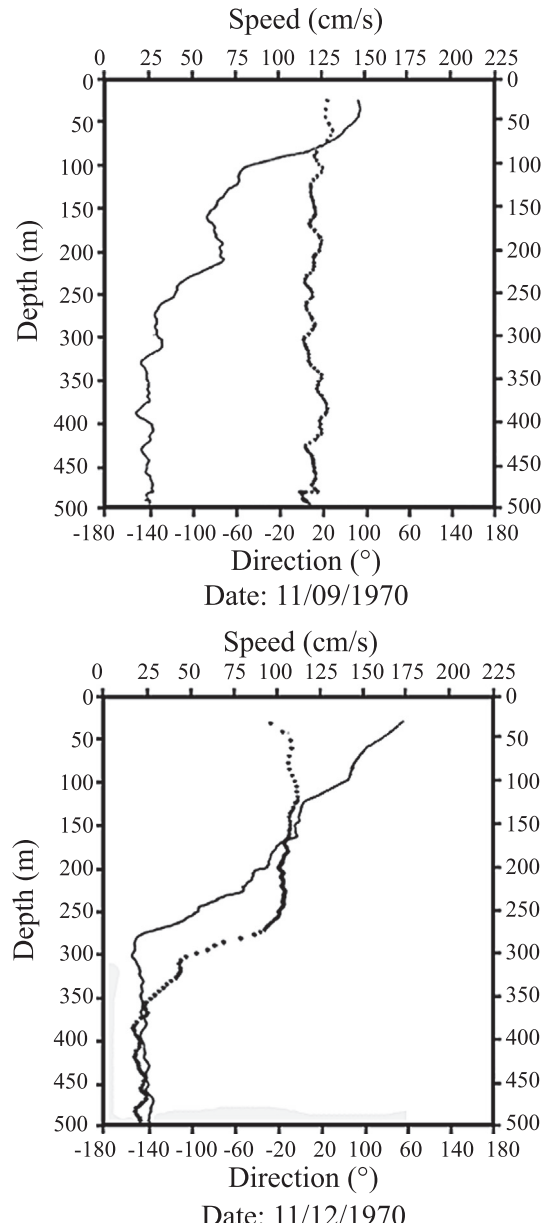


**FIGURE 10.2** Two selected profiles obtained using the PCM method, from the same location in the Florida Straits on two different months in the year 1970. (Source: Duing and Johnson, 1972.)

measure continuous profiles of horizontal current and temperature in small current regimes over long periods of time while unattended. It is reasonable to assume that vertical spacing of 10 cm should sample the mean properties of the velocity and density field sufficiently well to define a meaningful local Richardson number and yet not be unduly contaminated by the motions of the turbulent eddies.

One possible method of measuring vertical profiles of horizontal current and temperature with fine temporal and spatial resolution is the use of a slowly descending/

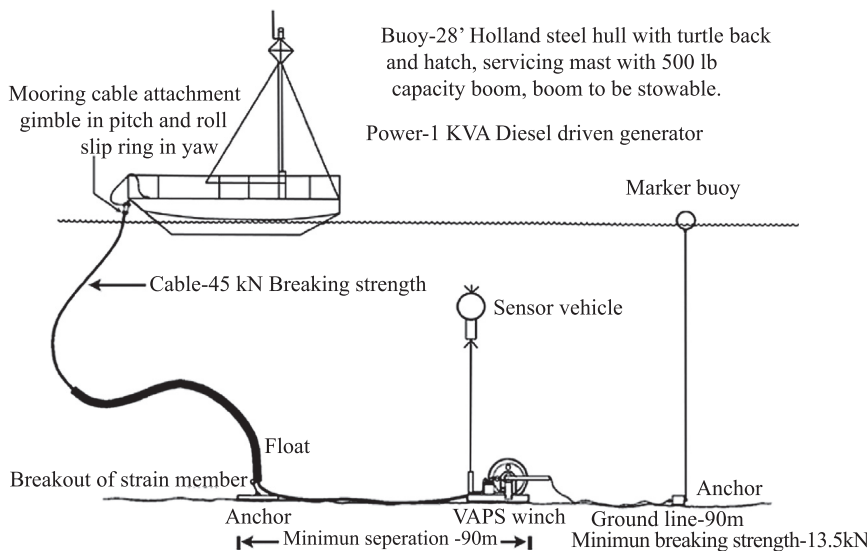


**FIGURE 10.3** Schematic of the VAPS system. (Source: Royer et al., 1987.)

ascending probe. The automatic profiling system (VAPS) reported by Ward-Whate (1977) consists of a buoyant sensor vehicle that carries a suite of sensors, capable of traversing 150 m of water column in the vertical via a lightweight tether cable and a bottom-mounted winch. A schematic of the VAPS system is shown in Figure 10.3. A 2-km-long cable from shore carries electrical power and control signals to the profiler system. X and Y components of current speeds, compass heading, time, depth, temperature, roll, and pitch signals are telemetered back to a recorder on shore.

The 360-kg bottom-mounted aluminum winch is powered through a regenerative (four-quadrant),  $\frac{1}{4}$ -hp, SCR-based speed controller located on shore. The drum speed is sensed by a tachometer and fed back to the shore-based controller, which corrects the ascent or descent rate to within several percent of the nominal values. The tether is wound onto a 64-cm-diameter drum, grooved in a single layer, which is guided by a level-wind assembly. Limit switches at the two ends of the level-wind assembly are preset manually to determine the reversing points of the winch. The reversing mechanism is controlled automatically by electronic logic circuits. The automated mode can be overridden manually to stop the float or to measure profiles at different rates or between various depth limits.

Connecting the winch and vehicle to shore is 2 km of 10-conductor, 2.5-cm-diameter cable, which is split on to two reels for easier deployment from a 28-m boat. The system is powered by either a conventional line source or an on-site generator. If power fails, the internal clock continues to function for about six days, a normal end-of-profile marker is recorded at shore, and the controller logic is set to begin a new profile starting at the bottom when the power resumes.

A standard 22-cm-diameter electronics canister mounts and interfaces the following sensors (Ward-Whate, 1977):

- **Current sensor.** Two-axis acoustic travel-time difference (ATT) type, mounted on the lid of the electronics can ( $\pm 100$  cm/s full scale with 0.1 cm/s sensitivity).
- **Direction sensor.** Optically scanned/encoded magnetic compass gimbaled; oil damped; 1 s recovery time;  $0-360 \pm 3^\circ$  with digital-to-analog conversion.
- **Depth sensor.** Strain gauge type;  $0-200 \pm 0.6$  m.
- **Temperature sensor.** High-purity, platinum-resistance thermometer; fast response; 0 to  $25 \pm 0.04^\circ\text{C}$ .
- **Tilt sensor.** Pendulum type; gimbaled; dual axis; oil damped; 1 s recovery time;  $45 \pm 1^\circ$ .

A 69-cm-diameter syntactic foam sphere surrounds the electronics package, giving a net positive buoyancy of 600 N (150 lb) force. This shape has been tow-tested and found to be stable in pitch, roll, and yaw at velocities up to 100 cm/s and has moderately low drag, thereby minimizing lateral drift.

The winch is lowered from a boat or pontoon tender suspended from a pivoting frame. Based on experience, the entire operation requires four people and three hours of calm weather.

Of paramount concern to a moving current sensor is the influence of self-motion on measurement accuracy. In all but shallow water moorings, the two-axis tilt sensor showed very little change ( $<1^\circ$ ). In shallow moorings, the following three effects have been found to dominate with increasing wave activity: (1) near the surface, wave particle motion is impressed on the current sensor; (2) the unsteady wave flow can initiate a yaw and roll instability in the vehicle as well as a surging action; this activity is at a high enough frequency that the compass readings become very erratic; and (3)

near-bottom wave motion can excite a pendulum-type oscillation of the body and tether above the winch.

An inherent limitation results from hydrodynamic effects due to the position of the current sensor atop the vehicle. Measurements are made on the up cycle only, and this constant upward velocity of the vehicle is added vectorially to the natural horizontal current. Lateral drift of the vehicle may be neglected due to the high buoyancy relative to the drag. The current sensor detects a simple, skewed resultant, which, in the case of low natural currents, impinges on the vehicle beneath, the presence of which displaces the flow streams through the measurement plane. The size and location of the current meter's acoustic mirror and its support posts add nonlinearly to output noise. Calibration of the current sensor, which is mounted on the vehicle, and the results obtained have been reported by Ward-Whate (1977). It has been found that the effective threshold for the vehicle-borne current sensor is 10 times its actual sensitivity of 1–2 mm/s, primarily because of its location atop the vehicle and its own physical shape.

Hamblin and Kuehnel (1980) successfully used this profiler for long-term unattended measurements of profiles of horizontal current and temperature at fine vertical resolution in a deep lake of moderate size (Kootenay Lake in British Columbia, Canada). Based on the excellent profiles they collected, it has been legitimately concluded that the disadvantages of the solid-state current sensor—namely, the care required to establish the environmental influences on the zero stability and gain and to establish its nonlinear calibration—are outweighed by its ability to detect the weak flows found in deep lakes that cannot be sensed by conventional mechanical devices on account of their high speed threshold.

Royer et al. (1986) conducted an intercomparison study of the VAPS in Lake Erie with drogues and current meters. Figure 10.4 shows a comparison between currents sampled by VAPS and currents measured at 21-m depth with a current meter at a nearby mooring. The agreement between the current speeds is extremely good, and, for most of the time, so is the agreement between the current directions. The few cases in which the directions disagree correspond to times of such low velocity that the directional thresholds of the fixed CM are being approached. According to Royer et al. (1986), the correspondence between instruments at 10-m depth is also as convincing as the one at 21-m depth for speeds above 2.2 cm/s, which is the threshold speed of the Plessey current meter.

Figure 10.5 shows a comparison between currents sampled by VAPS and currents measured with drogues at 3-m depth. The velocities can be extracted from successive positions and corresponding times of each drogue. A comparison of Lagrangian drift to an Eulerian current is strictly valid only for a uniform flow, but it is reasonable to expect that horizontal uniformity in the comparison

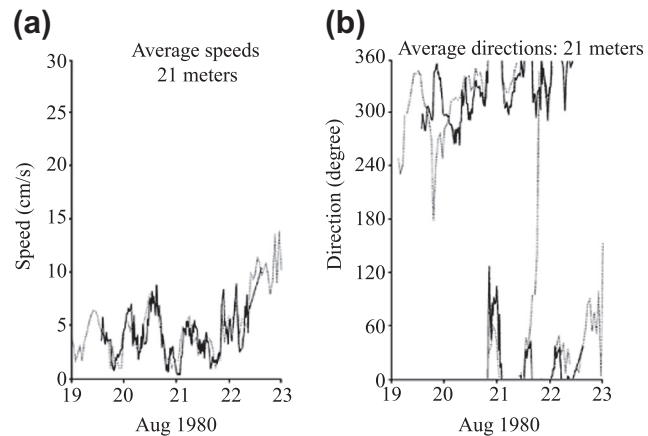


**FIGURE 10.4** Comparison between currents sampled by VAPS (solid line) and currents measured at 21-m depth (dotted line) with a Geodyne current meter at a nearby mooring. (a) Compares speed; (b) compares direction. (Source: Royer et al., 1986.)

experiment reported by Royer et al. (1986) would be sufficient to allow comparison of the resulting drogue speeds and directions to the VAPS data as being characteristic of the whole area. The drogues chosen for the comparison were usually closer to the VAPS site; therefore, the good correspondence between the speeds and directions of the two current estimators is not surprising. The near-surface speeds are usually higher than those at lower depths, thus giving rise to a better definition of the direction of the current.

The successful comparison with conventionally measured currents and temperatures establishes that these parameters can be accurately measured from a moving profiler in an exposed large water body. The agreement between the uppermost VAPS current and the surface wind field suggests that the profiler would be capable of resolving the surface and bottom boundary layers, provided that some way could be found to maneuver the sensors more closely to the surface and bottom.

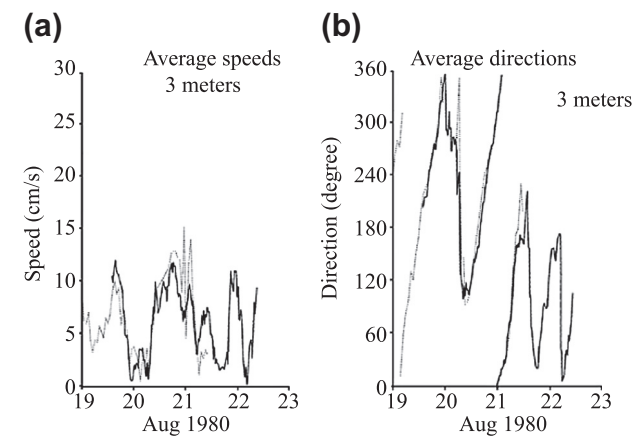


**FIGURE 10.5** Comparison between currents sampled by VAPS (solid line) and currents measured with drogues (dotted line) at 3-m depth. (a) Compares speed; (b) compares direction. (Source: Royer et al., 1987.)

The VAPS record provided a fascinating glimpse of the intimate coupling between the temperature and velocity distributions in Lake Erie. In particular, the velocity profiles indicated a surface current swinging in direct response to the observed winds. It was also observed from the VAPS vertical profile measurements that “transient” thermal structure exerts an important influence on the distribution of momentum during periods of relatively light winds, which is an observation in agreement with that reported by Price et al. (1986). The VAPS measurements provided a clear indication that only during periods of very strong winds does Lake Erie assume a truly two-layered structure. The tantalizing glimpse of the richness and variety of the subsurface velocity and temperature structure suggests that only the data from a profiling instrument can adequately resolve the structural details of a current regime.

### 10.2.3. Acoustically Tracked Freely Sinking Pingers

The pinger-tracking method used for measurement of vertical profiles of horizontal currents in the deep ocean is the oceanic analog of the meteorological pilot balloon. The acoustic method obtains a current-velocity profile from the acoustical determination of the trajectory of a free-falling probe. In this method, an instrument package containing an acoustic pinger is ballasted to descend to the ocean floor, where it can be released by an acoustic release mechanism, a corrodible link, or a preset timed-release mechanism controlled by the electronics in the instrument package. The pinger’s trajectory is determined by acoustically tracking it relative to an array of at least three units of spatially separated surface- or bottom-moored acoustic transponders.

While the pinger slowly descends to the seafloor and then ascends to the surface, it transmits a continuous-wave (CW) pulse (i.e., an acoustic ping of a few milliseconds’ temporal width) at selected time intervals. On reception of the ping, the transponders reply at separate frequencies. The round-trip travel time of pulses between the pinger and each transponder (i.e., the time elapsed between the interrogation and reply pulses) is recorded in the electronics package of the pinger. From the different round-trip travel times, the trajectory of the pinger in three-dimensional space is determined. As the pinger falls and rises, it encounters a variety of forces that result from its relative velocity with respect to the surrounding water mass. The vertical profile of horizontal flow velocities is estimated from the horizontal displacements of the freely falling or rising pinger relative to the moored transponders. Thus, from the tracking data, it is possible to compute the horizontal velocity as a function of depth.

Rossby (1969) described an experiment to measure the overall vertical profile of horizontal ocean currents on the southern slope of Plantagenet Bank southwest of Bermuda

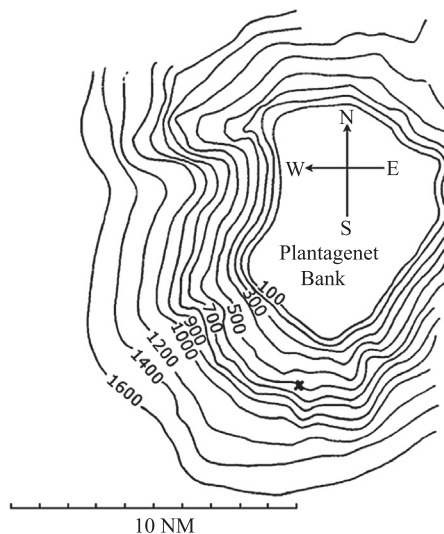


**FIGURE 10.6** Portion of topography around Plantagenet Bank with contour lines shown at 100-fathom intervals. The Bank is situated 25 nautical miles (NM) southwest of Bermuda. The sinking float was released at the point marked by a cross. (Source: Rossby, 1969.)

(see Figure 10.6) while retaining high resolution of the small-scale structure by tracking acoustically a slowly sinking pinger (a standard Swallow float). The float, equipped with slanted vanes causing it to rotate as it sinks, was released from a research vessel. The design for rotation was meant to eliminate or considerably reduce any inherent tendency for the float to veer or coast in any preferred direction. The particular location for the experiment was dictated by the existence of a set of hydrophones on the southern slope of the Bank.

The successive positions (i.e., three-dimensional geographical coordinates) of the free-falling pinger were determined based on a principle that is somewhat analogous to that used for position fixing (i.e., determining the precise position) of a ship surveying in the offshore regions. Before the advent of the now ubiquitous GPS, the geographical coordinates of a survey ship were determined based on the known positions of a navigation transit satellite (i.e., a satellite that passes overhead) in near-polar orbit at an altitude of  $\sim 1,100$  km and with an orbital period of  $\sim 107$  min, moving at a speed of  $\sim 20,000$  km/h. In this satellite navigation (SatNav) scheme, a given navigation satellite transmitted a set of signals at successive discrete time intervals and a Doppler Navigation System receiver located in the ship received the signals when the satellite remained on the horizon. The position fixing of the ship was accomplished based on an estimate of the intersection of the two surfaces of the space hyperboloid (constructed from the successive range differences between the satellite and the ship) with the sea surface, and judiciously choosing one of the two mathematically admissible locations of the ship, the alternate location being on the other side of the

track swept by the satellite's footprint on the surface of the Earth (Joseph, 2000).

Position fixing of the free-falling pinger, based on the principle of construction of a hyperboloid as indicated, requires determination of successive range differences between the pinger and a two- or three-dimensional array of spatially distant hydrophones located on the seafloor. This is because hyperbolae are loci of constant differences in distance to two points. The float (i.e., pinger) used by Rossby periodically transmitted a ping, which was received by four hydrophones located on the seafloor. The theory for tracking is as follows: Assume that the four receivers have the locations  $(x_i, y_i, z_i)$ , where  $i = 1, 2, 3, 4$ . The distances  $r_i$  from the pinger at  $(x, y, z)$  to the receivers are  $((x - x_i)^2 + (y - y_i)^2 + (z - z_i)^2)^{1/2}$  and are equal to the effective sound speed  $v_i$  times the travel time  $t_i$ . Assuming that the effective sound speeds  $v_i$  are the same and known, it is possible to construct three difference equations to be solved for the three unknowns  $x$ ,  $y$ , and  $z$  from the four range equations (note that  $i = 1, 2, 3, 4$ ):

$$v_i^2 t_i^2 = ((x - x_i)^2 + (y - y_i)^2 + (z - z_i)^2)^{1/2} \quad (10.4)$$

In practice the solution is obtained by an iterative procedure. Allowance is made for the variation in effective sound speed, which corrects for ray bending and is defined as the equivalent sound speed for an acoustic signal along a straight path. It can be computed from knowledge of the vertical sound-velocity profile, together with the angle from the vertical of the equivalent straight ray. Expansion of Equation 10.4 yields the following:

$$\begin{aligned} v_i^2 t_i^2 &= x^2 - 2xx_i + x_i^2 + y^2 - 2yy_i + y_i^2 \\ &\quad + z^2 - 2zz_i + z_i^2 \end{aligned} \quad (10.5)$$

Putting  $i = 1$  in Equation 10.5 yields the following:

$$\begin{aligned} v_1^2 t_1^2 &= x^2 - 2xx_1 + x_1^2 + y^2 - 2yy_1 + y_1^2 \\ &\quad + z^2 - 2zz_1 + z_1^2 \end{aligned} \quad (10.6)$$

Determination of range differences for construction of hyperbolae (which is a requirement for determining the successive positions of the free-falling pinger in three-dimensional space) can be accomplished by forming three difference equations. This can be achieved by subtracting Equation 10.5 from Equation 10.6. Accordingly, Eq. (10.6) – (10.5) and appropriate rearrangement yields the following expression:

$$\begin{aligned} 2x(x_i - x_1) + 2y(y_i - y_1) + 2z(z_i - z_1) \\ = (x_i^2 + y_i^2 + z_i^2) - (x_1^2 + y_1^2 + z_1^2) \\ - v_i^2 t_i^2 + v_1^2 t_1^2 \end{aligned} \quad (10.7)$$

where  $i = 2, 3, 4$ , and  $x, y, z, t_1, t_2, t_3, t_4$  are unknown. However,  $t_i$  can be expressed as  $t_1 + (t_i - t_1) = t_1 + \Delta t_i$ , where  $\Delta t_i$  are the measured time differences. If these are substituted into the three equations, we have three unknowns  $(x, y, z)$  as a function of  $t_i$ . The solution is found by assuming a value for  $t_1$  and perturbing it until a set of coordinates  $(x, y, z)$  is found, which, when inserted into the four range equations, will yield the same time differences as those measured. In a three-dimensional situation, with the slowly sinking float (i.e., the transmitter) hanging in the ocean and the four spatially separated hydrophones (i.e., receivers) fixed on the seafloor, the slant-range differences (equivalently, the measured time differences) define a hyperbolic surface. The transmitter can be anywhere on the surface of the hyperboloid. Thus, there is more than one solution to the problem, but only one solution will satisfy the expectation that the transmitter be at a reasonable point in the water and not in the Earth's crust or atmosphere!

In the method adopted by Rossby (1969), two passes are made through the data. In the first pass,  $(x, y, z)$  as a function of time are obtained. In the second pass, the depth is treated as a known smooth function of time and only  $(x, y)$  are computed. This permits one to select the best three of four receivers for the final calculations. The only assumption made is that the float sinks at a steady rate. Systematic and random errors affect the accuracy of the velocity estimates. The errors are those associated with the acoustic navigation of the pinger and those involved with the interpretation of the horizontal velocity of the pinger as oceanic motion. Some sources of possible errors in the position estimates are (Rossby, 1969):

- Uncertainty in timing resolution
- Amplification of errors by the geometry of hyperbolae
- Variation in effective sound velocity due to internal waves
- Uncertainty of the sound-velocity profile and receiver locations

Of these, the first two are the most significant. In Rossby's experiment, the time difference to 0.1 ms was measured. Advancement in electronics technology easily reduces such uncertainties.

The difficulty associated with the hyperbolic geometry is that hyperbolae are loci of constant differences in distance to two points. Given a distance difference with a certain possible error, the error band for the locus will grow rapidly as the distance from the axis between the two points increases or if the solution lies close to the baseline extension between the two points. The result of these two errors is that for each of the time differences, two time measurements are required, both of which introduce timing errors that together become amplified if the solution is far from the baseline of the receivers. The error arising from variation in effective sound velocity is believed to be minor

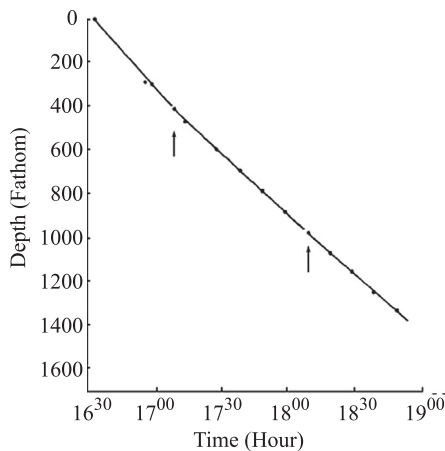


**FIGURE 10.7** Depth of the float as a function of time. It is approximated by three linear sections for the purpose of ease in analysis. (Source: Rossby, 1969.)

as long as the acoustic ray has not been totally refracted. In this case there is little scatter and a single path arrival is achieved. Internal waves will perturb the path. However, if the mode number is high, the combined effect should remain small. Also, if the thermocline as a whole moves up or down, the resulting change in effective sound speed is estimated to be less than 1 m/s. The consequence of change in travel time arising from this change in effective sound speed is considered negligible. Uncertainty of the sound-velocity profile can be minimized by knowing the water-temperature profile in the region of interest, because the sound-velocity profile can be estimated from the measured or known temperature profile.

A depth-versus-time curve for the float, approximated by three linear sections and obtained from the first analysis of the tracking data, is shown in Figure 10.7. The sinking rate was about 17.5 cm/s. The second analysis gave the results shown in Figure 10.8, in which the trajectory is composed into its north-south (N-S) and west-east (W-E) components. In interpreting this figure, it must be borne in mind that the horizontal velocity at any depth is given by the deviation of the trajectory from the vertical. The nomogram in the center of the figure gives the velocity as a function of angle. Similarly, the curvature of the trajectory is a measure of the vertical shear. In principle it is obtained from the second derivative  $\frac{d^2}{dz^2}$  of the trajectory. In practice it is difficult to measure this quantity, because it is limited to thin regions where the velocity changes almost discontinuously.

The dots along the trajectory are the computed positions of the float at one-minute intervals. Although the ping repetition rate was one every 2.4 s, the times of arrivals were averaged in 15-s groups from which the float position was calculated. It is evident from the trajectory in Figure 10.8 that high velocities dominate from the surface

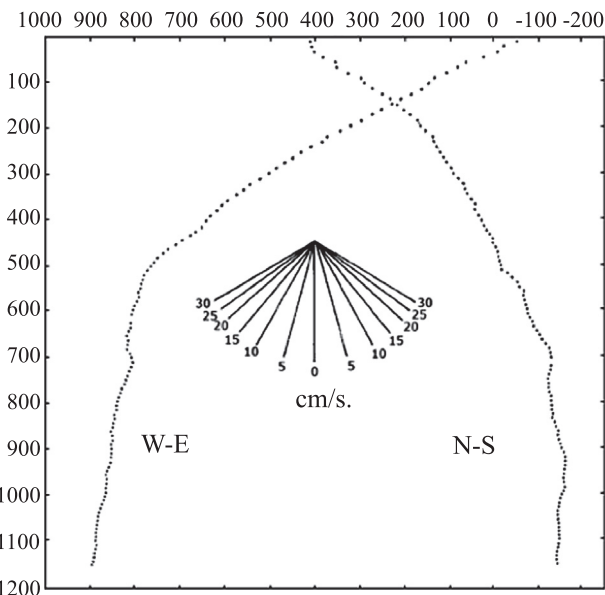


**FIGURE 10.8** The trajectory of the float separated into its N-S and W-E components as a function of depth. The horizontal velocity at any depth is obtained from the slope of the trajectory and the nomogram in the center of the figure. The vertical scale is in meters from the sea surface and the horizontal scale is in meters N-S or W-E with respect to an arbitrary origin. The dots indicate the position at one-minute intervals. (Source: Rossby, 1969.)

down to the upper limit of the main thermocline, where there is a sudden transition to slowly moving deep water. Rossby (1969) proposes that it is not possible to state with certainty whether this transition is typical of the flow far from the Bank or whether it is peculiar to the flow around the Bank. According to Crease (1962), such low velocities are not typical of deep water in the Sargasso Sea. According to the profile measurements by Rossby (1969), the deep water appears to be moving to the west, suggestive of a weak tangential flow along the bottom topography. Based on several hydrographic measurements and current profile measurements, it is inferred that the Bank has a pronounced influence on the water-current flow in its vicinity.

The abrupt change in N-S flow at 510 m corresponds to a velocity difference of 20 cm/s. It is inferred that this particular high shear zone is an interface between turbulent patches of water agitated by the flow around the Bank. Noteworthy information that could be gleaned from the profile measurements of Rossby (1969) is poor indication of the regularly spaced steps reported by Cooper and Stommel (1968) in this region.

In an analysis by Rossby and Sanford (1976), the trajectories in the vertical and east plane and the vertical and north plane during an interval of 200 s are separately fitted in a least-squares sense to parabolic curves. The fitted curve is differentiated with respect to time to

determine the east, north, and vertical-velocity components of the probe's motion. It is assumed that the horizontal velocity components of the float are equal to those of the surrounding water. The rms difference between the measured and fitted trajectories is typically 1 m. Thus, if the instrument is sinking at 0.25 m/s in the presence of a 0.10 m/s horizontal current, it will be advected 20 m horizontally during a 50 m vertical interval. According to Rossby and Sanford (1976), a single end-point determination of the advection rate without any curve fitting would lead to a maximum 10 percent, or 0.01 m/s, uncertainty in horizontal speed. The least-squares curve fit reduces this level of expected error.

#### 10.2.4. A Freely Sinking and Rising Relative Velocity Probe (Cyclesonde)

Van Leer et al. (1974) reported the design and use of a vertically scanning instrument package called the Cyclesonde (see Figure 10.9). The Cyclesonde derives its name from the fact that it profiles the upper ocean periodically, in much the same way as a radiosonde station profiles the lower atmosphere. Furthermore, both these tools are buoyancy-driven systems.

The Cyclesonde consists of a gas-operated, buoyancy-driven probe with a recording package containing sensors for measurements of water-current velocity, temperature, and depth. It makes repeated automatic round trips up and down a taut-wire subsurface mooring at selected vertical speeds of between 2 and 20 cm/s while scanning the horizontal currents at successive depth layers. The combination of a ball-bearing roller block and smooth plastic-coated wire gives a low coefficient of friction ( $\mu$ ) of about 0.02 on the wire, with no noticeable increase in friction for periods of immersion of a week or more. A block designed with three overlapping wheels prevents the plastic wire from chafing on the block's cheeks and reduces friction.

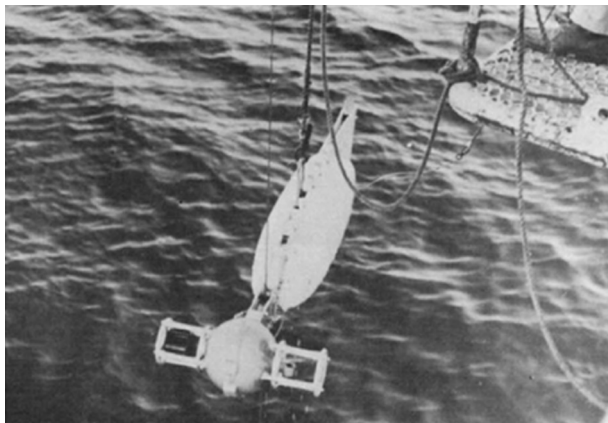


**FIGURE 10.9** A complete Cyclesonde being deployed for ocean-current profile measurements. (Source: Van Leer et al., 1974.)

This block opens on one side to allow the Cyclesonde to be removed from the wire without breaking the wire. A safety wire holds the wire, sphere, block, and hull together. The Cyclesonde's motion is controlled by ballast, buoyancy, and drag adjustments.

The sensors (water-current velocity, temperature, and pressure) are located in two protecting cages mounted symmetrically on both sides of an aluminum ball on the head of the Cyclesonde. The side location gives the sensors unobstructed exposure for both the up and down profile of each round-trip cycle. A variable buoyancy device (VBD) package and a scuba tank of the Cyclesonde trail downstream of the taut wire, enclosed in a low drag (drag coefficient  $C_D = 0.7$ ) plastic hull that acts as a 1.5-m-long current vane. The long vane greatly reduces vane flutter due to wave and mooring motion. The hull orients the current speed sensor (Savonius rotor) so that the vector sum of the vertical speed of the Cyclesonde and the horizontal component of current lies in a plane perpendicular to the rotor's axis of rotation. The whole Cyclesonde, including the magnetic compass for current direction measurement, turns with the vane, and thus no vane follower is required for speed-direction estimation. The device measures and records these parameters as a function of time. The use of the unattended Cyclesonde on a taut-wire mooring is limited to current regimes with speeds of less than 90 cm/s.

The Cyclesonde may be operated from a ship or deployed on a mooring. When a ship is anchored in a region where currents are less than 2 knots (1.02 m/s) or it is drifting slowly, a Cyclesonde will run up and down a ship-lowered wire held taut by a heavy weight. Because the wire is run in or out only when the Cyclesonde requires service, a crude winch or capstan is sufficient, freeing the winches for other sampling programs. Several hundred profiles of current speed and direction, temperature, and depth have been recorded in this mode of operation.

When the Cyclesonde is deployed on a mooring, the device is constrained by a closed pulley to ride up and down a smooth plastic-coated wire (about 4-mm diameter). The wire is held taut between a seafloor-mounted anchor weight (e.g., a railroad wheel) and a subsurface float of  $\sim 350$ -lb buoyancy to minimize the wire angle  $\theta$ . At the bottom of the wire there is an auxiliary float and a weak link. Should the anchor become fouled, the weak link will break when the mooring is recovered, thereby saving the Cyclesonde wire from breaking. A ground-line auxiliary anchor and slack-wire surface float may be used in typical continental shelf depths. If the weather permits, divers may exchange Cyclesondes in a short period of time, giving minimum data interruption. Using this technique, Van Leer and colleagues (1974) regularly serviced Cyclesonde moorings in an hour in 80-m water depth, and several hundred profiles were made on moorings in the Gulf of Mexico and Oregon shelf regions.

### 10.2.4.1. Operation

The Cyclesonde's cyclic vertical motion is controlled by changing the mean density of the instrument package a few percent. These density changes are accomplished by an inflatable bladder, which is used to change the displacement of the Cyclesonde so that its buoyancy is made negative at a pre-selected low pressure and positive at a pre-selected high pressure. This causes the instrument package to cycle between these two specific water pressures. The original design covers a maximum depth of 200 m. Figure 10.10 shows the variable buoyancy device. Its component parts are an aluminum scuba tank, pressure regulator, deep valve, differential pressure valve, shallow valve, and bladder assembly (see Figure 10.11). The swim bladder assembly, shown in Figure 10.10, consists of a rubber tube closed at one end and fastened to an inlet port at the other. The tube is placed over a PVC rod to maintain its volume when deflated. The swim bladder is enveloped by a Plexiglas tube so that its inflated dimensions are the

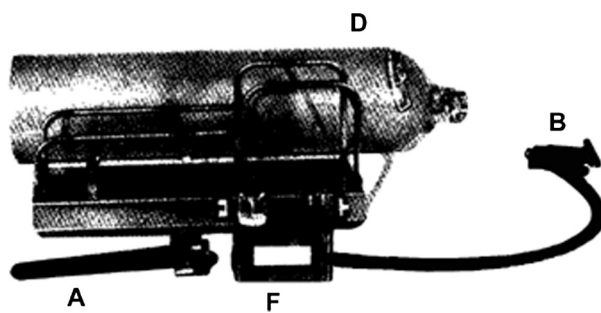


**FIGURE 10.10** Variable buoyancy device. A: Swim bladder. B: Tank regulator valve. D: Scuba tank. F: Differential pressure valve. (Source: Van Leer et al., 1974.)

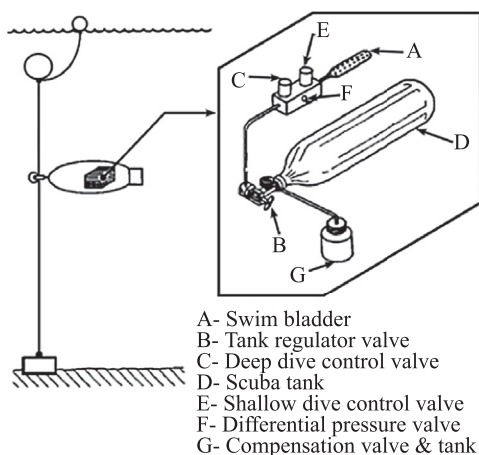


**FIGURE 10.11** Principal parts of the variable buoyancy device. A: Swim bladder. B: Tank regulator valve. C: Deep-dive control valve. D: Scuba tank. E: Shallow-dive control valve. F: Differential pressure valve. G: Compensation valve and tank. (Source: Van Leer et al., 1974.)

same for each inflation. The neoprene bladder can be inflated to 400 cm<sup>3</sup>.

The variable buoyancy device is powered by compressed helium contained in an aluminum scuba tank. Aluminum was chosen because of its lightweight and nonmagnetic properties. A Décor Model 300 first-stage regulator valve was modified to maintain a pressure of 25 psi ±10 over the ambient water pressure to inflate the bladder. A detailed drawing of the valve assembly is shown in Figure 10.12. The stainless-steel heads of the deep and shallow control valves protrude from the valve body and are used to set the upper and lower turnaround pressures. Each of the control valves has a calibration curve of turns versus pressure that is used for accurately selecting the turnaround depths.

Six ports,  $P_1$  to  $P_6$ , are drilled into the valve body.  $P_1$  allows gas to enter the control valve assembly from the regulator,  $P_2$  supplies gas at a controlled pressure to the swim bladder, and  $P_3$  to  $P_6$  are vented to the seawater. A deep turnaround depth between 0 and 200 m and a shallow turnaround between 0 and 26 m can be selected without changing the spring. To prevent overpressure inside the swim bladder during ascent, a pressure-relief valve opens to  $P_4$  when the pressure differential across the swim bladder and seawater exceeds 37 psi.

A loss of gas occurs each time the gas in the bladder is expelled to the sea. Because of its low molecular weight, helium was used to minimize the changes in trim arising from this loss. Up to 300 cycles can be obtained using helium before weight compensation becomes necessary.

A complete Cyclesonde system is composed of the following components: (1) a variable buoyancy device (VBD), (2) mooring or ship-lowered wire, (3) an instrument package, (4) a pulley block, and (5) propulsion housing. In a successful Cyclesonde system, the change in buoyancy,  $\Delta B/2$ , must always exceed that portion of the

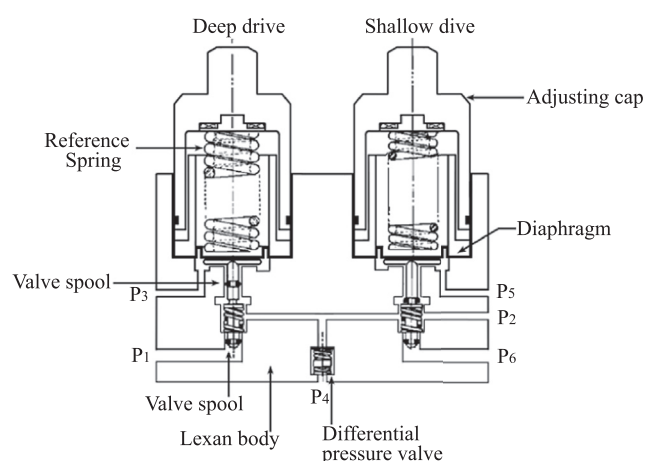


**FIGURE 10.12** Valve body arrangement. (Source: Van Leer et al., 1974.)

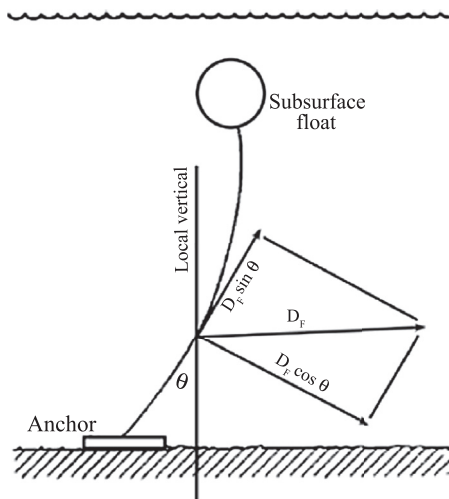


**FIGURE 10.13** Schematic diagram of acting forces. (Source: Van Leer et al., 1974.)

drag force acting along the wire plus the component perpendicular to the wire, multiplied by the coefficient of friction of the roller running on the wire (see Figure 10.13). Thus, the condition to be satisfied is the following:  $(\Delta B/2) > D_F (\mu \cos \theta \pm \sin \theta)$ , where  $\Delta B$  is the buoyancy change due to the swim bladder;  $D_F = (C_D A \rho / 2) V_H^2$ ;  $\theta$  is the wire angle, and  $\mu$  is the coefficient of friction.  $A$  = Cyclesonde frontal area;  $V_H$  = horizontal velocity;  $C_D$  is the horizontal drag coefficient; and  $\rho$  is the local seawater density. The sign of the sine term depends on whether the direction of travel is the same as the direction of the drag component acting along the wire.

For a moored Cyclesonde, the surface or subsurface float usually trails downstream (see Figure 10.13) so that the component of drag in the layer of strongest current acting along the wire usually acts to oppose the friction force when the Cyclesonde moves upward. The friction force always acts to oppose the motion. Because the horizontal velocity component  $V_H$  and the local seawater density  $\rho$  are determined by the ocean, the variables available to the designer are  $C_D$ ,  $A$ ,  $\mu$ , and  $\theta$ . To make  $C_D A$  as small as possible, the displacement of the Cyclesonde must be minimized. Each kilogram of excess wet weight in the instrumentation or VBD system must be supported by about 2 kg of syntactic foam, giving a total increase in the displacement of about 3 kg. The additional area added by such an increase in Cyclesonde displacement is multiplied by the square of the velocity. This aspect of the problem results in a greater drag force, which must be overcome by increasing the change in buoyancy ( $\Delta B/2$ ) used to move the Cyclesonde vertically. For a given number of profiles, the gas supply would need to be increased, which again increases the volume displaced. To avoid this “snowballing” effect of increasing total displacement, every possible effort must be made to keep the component weight to a minimum.

Based on field experience, some modifications in the design became necessary. For example, the VBD had to be used with some modifications as follows: The heavy stainless steel mounting frame had to be omitted to save weight. Surgical rubber tubing was substituted for the neoprene swim bladder to extend bladder life to approximately 300 inflations using a displacement of  $\Delta B = 600 \text{ cm}^3$ . A new longer-life swim bladder using toroidal geometry, developed at the University of Miami, survived without failure for over 5,000 inflations (at  $600 \text{ cm}^3$ ) in a prototype model (Van Leer et al., 1974).

Because the axis of rotation of the Savonius speed sensor is horizontal, it responds with equal sensitivity to both the horizontal current speed and the vertical motion of the Cyclesonde. This means that the vertical velocity of the Cyclesonde must be subtracted from the observed speed. This is done by using the rate of change of water pressure with time as a vertical velocity estimate. One advantage of the sensitivity of the horizontally mounted Savonius rotor to the sum of the horizontal current speed and the vertical motion of the Cyclesonde is that the rotor operates outside its nonlinear threshold region. Figure 10.14 presents unedited, unsmoothed raw data in the format of time series as recorded by the Aanderaa current meter, which formed the sensing and recording device of the Cyclesonde. Figure 10.15 presents unsmoothed, original vertical profile observations obtained during February 1973 in the Gulf of Mexico.

#### 10.2.4.2. Advantages

A noteworthy advantage of the Cyclesonde is that the roller decouples the Cyclesonde from the vertical heaving motions of a ship or mooring. This makes relatively noise-free measurements possible because the measuring instrument moves slowly, smoothly, and monotonically through the water. Noise problems such as “salinity spiking” and “rotor pump up” are much reduced relative to conventional techniques. Furthermore, the Cyclesonde has nearly a cosine response to currents not in the plane of the fin (hull), as a result of which horizontal wave-induced mooring motions perpendicular to the fin tend to average. This leaves the fore and aft motions (in the plane of the fin) of the mooring as a major source of wave-induced rotor error.

In regions of weak currents, Cyclesonde measurements from taut-wire, subsurface moorings are preferable to ship-lowered measurements because of uncertainties introduced by the ship’s motion on its anchor, the ship’s changing magnetic influence on the compass used in the current meter, and the ship’s effect on flow in its immediate vicinity. The magnetic properties of a Cyclesonde mooring must be given special consideration because the instrument can move close to the iron anchor and subsurface float. The large hull makes a very sensitive vane, allowing accurate

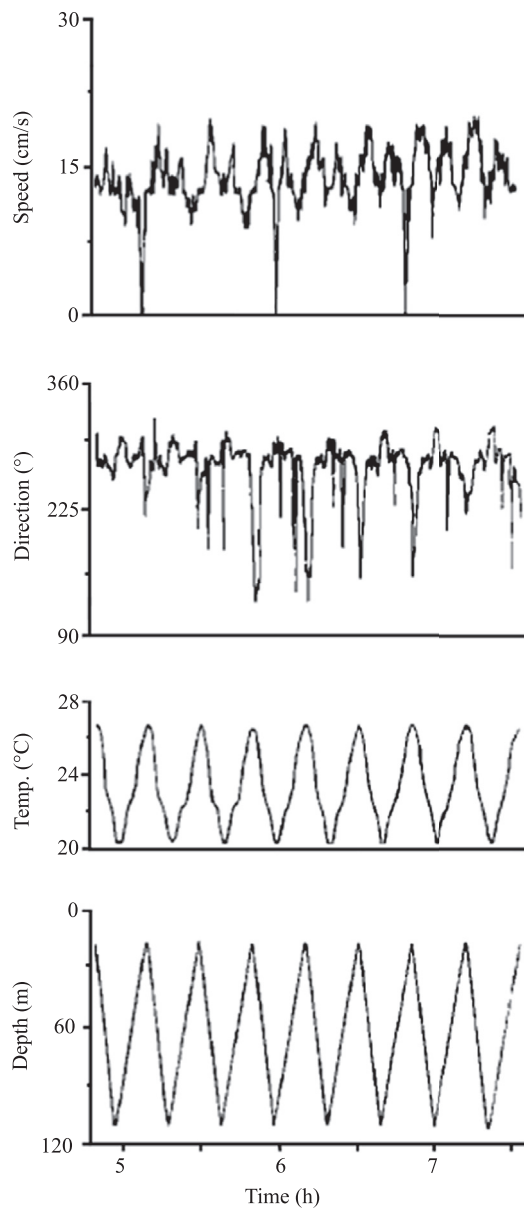


**FIGURE 10.14** Original records collected by Cyclesonde. (Source: Van Leer et al., 1974.)

current-direction data at very small horizontal water speeds. Evidence for this was found by Van Leer et al. (1974) in their shallow-water tests in a protected region. Limitations of Cyclesonde include its limited vertical range and limited life for a given design.

### 10.2.5. A Freely Falling Electromagnetic Velocity Profiler

Various methods have been employed to determine the vertical profile of horizontal current  $V(z)$  at depth  $z$ . One approach, based on the measurement of motionally induced electric effects, was developed by Drever and Sanford

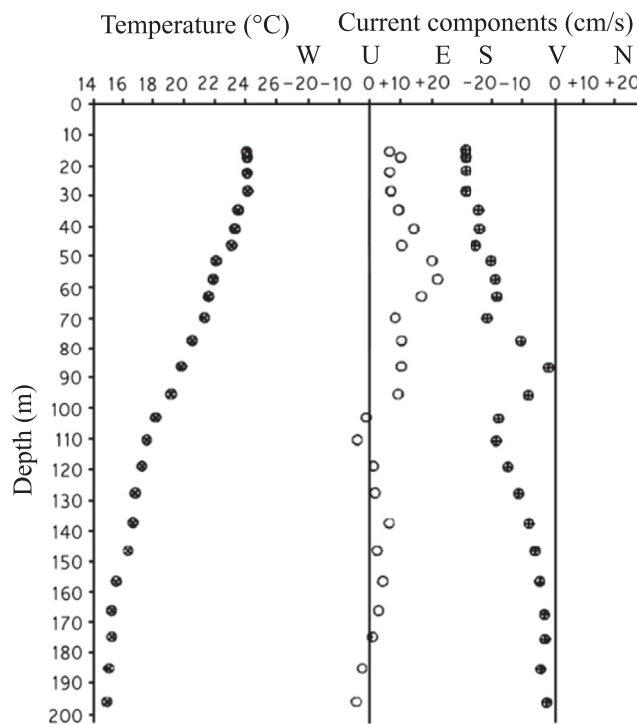


**FIGURE 10.15** Unsmoothed, original vertical profile observations obtained by Cyclesonde during February 1973 in the Gulf of Mexico. (Source: Van Leer et al., 1974.)

(1970). They showed that the weak electric fields and currents generated by the motion of the seawater through the geomagnetic field could be measured and related to the velocity profile. The instrument measures the voltages induced by the motion of the sea and the instrument through the geomagnetic field. The electric field is interpreted in terms of ocean-current velocity. Comparisons with an acoustically tracked probe demonstrated the electromagnetically inferred velocity profile to be accurate to about  $\pm 1$  cm/s (Rossby and Sanford, 1976). Sanford et al. (1978) developed an improved technique to determine the variations of horizontal flow velocity between the sea surface and the seafloor based on the measurement of electric currents generated by the motion of the seawater through the Earth's magnetic field. In this device, a freely falling *electromagnetic velocity profiler* (EMVP) senses the currents as a function of depth. The device is released from the surface, falls to a preset depth or to the seafloor, and then returns to the surface. Both descent and ascent take about 90 min in water 6,000 m deep. The design requirements of the EMVP were the following (Sanford et al., 1978):

- Velocity resolution of 1 mm/s, to observe fine structure
- Fall speed of about 1 m/s, for rapid profiling
- Rotation rate of once each 5 to 10 seconds, to separate motional signal from electrode offset
- Real-time acoustic telemetry and tracking

- Depth capability to 6000 m
- CTD functions
- Internal digital storage
- Rugged construction
- Orthogonal electric measurements every  $\frac{1}{2}$  s, for redundancy and fine vertical resolution
- Autonomous release from the sea surface
- Recovery aids including radio, flashing light, and acoustics

The EMVP differs from conventional electromagnetic (EM) current meters in that the geomagnetic field, rather than a locally generated magnetic field, is utilized. The response of the EMVP results from the motion of seawater relative to the geomagnetic field, whereas the EM current meter responds to the motion of water relative to its own magnetic field. In a sense, the geomagnetic field establishes a reference frame and the electrical response arises from motion relative to this reference. The physics of motional induction was discussed by Longuett-Higgins et al. (1954).

The EMVP is allowed to free-fall and is advected horizontally by the local flow velocity  $V(z)$  at depth  $z$ . It thus records a potential difference  $\Delta\phi = B \times (V(z) - \bar{V}^*)$ , where  $B$  is the local magnetic flux density of the Earth, and  $\bar{V}^*$  is the barotropic (largely depth-independent) contribution to the current. The local magnetic field of the Earth is available from the world magnetic field charts. The EMVP yields a profile in the form of  $[V(z) - \bar{V}^*]$  (Sanford, 1971). In the expression  $\bar{V}^*$ , the overbar denotes the vertically averaged character of the quantity. The asterisk denotes that there is an electrical conductivity weighting involved and that other contributions exist. In the EMVP, the electric current is measured as the voltage difference between two points on opposite sides of a vertical, insulating cylinder. The use of a large diameter outer skin not only increases the electrical sensitivity but also provides room inside for the electrodes, electronics pressure vessel, and floatation. In addition, by keeping the length down and the body streamlined, the profiler vehicle (see Figure 10.16) is easier to handle at sea. The vehicle is built up around a 7,075 aluminum alloy tube, 5 ft (1.52 m) long, with an outside diameter of 7.5 in (19.1 cm) and wall thickness of 0.75 in (1.91 cm). The tube and end caps are designed to withstand a pressure equivalent to 6,000 m.

The forward half of the tube is surrounded by five discs of syntactic foam, each of which has buoyancy in seawater of about 10 lb (4.5 N). Covering the foam and the remaining tube is a 14-in. (35.6-cm) cylindrical medium-density polyethylene shell, 0.25 in. (0.64 cm) thick. Beneath the lower portion of this shell are electrode housings connected by hollow plastic tubes to four holes equally spaced around the circumference (see Figure 10.17). A collar holding eight pitched fins, which

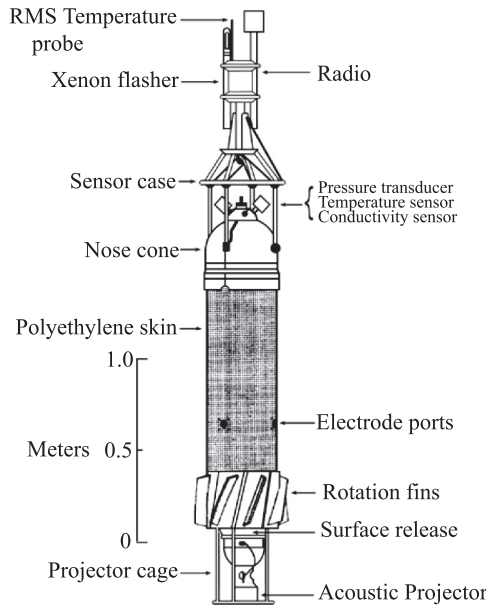


**FIGURE 10.16** Free-fall EMVP vehicle. A balloon keeps the profiler on the surface until the preset time when it is released by the surface release mechanism and the profiler begins its down profile. (Source: Sanford et al., 1978.)

cause the instrument to rotate as it falls, is mounted over the lowest part of the skin. Cages are attached to each end of the tube to protect the sensors and to provide places to lift and handle the probe. On the upper end of the sensor cage are mounted the recovery aids: a radio transmitter and a xenon flasher. These units are self-contained, having no electrical connection with the main instrument.

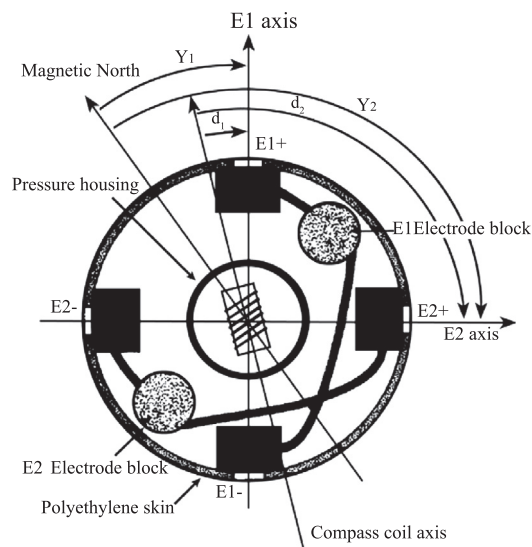


**FIGURE 10.17** Cross-section of the free-fall EMVP vehicle at the level of the electrodes showing the arrangement and orientation of the electrode arms (E1 and E2) and compass coil (CC). (Source: Sanford et al., 1978.)

Between the radio and flasher is a thermistor bead that is used to sense the high-frequency variations (0–16 Hz) of seawater temperature. The assembly is mounted on a frame that is able to flex relative to the sensor cage. An extra 13 N (30 lb) of expendable weights overcomes the positive buoyancy of the instrument (6.5 N) and forces it to fall toward the bottom. The weights are released either on contact with the bottom or at a preset depth. The release mechanisms are similar to those used by Richardson and Schmitz (1965). As a safety measure, a small corrosive magnesium link is placed between the release mechanism and the weights. During a 5,000-m drop, the fall and rotation rates gradually change by about 8 percent because of changes in buoyancy and viscosity. The ratio of fall and rotation rates changes by only 3 percent.

The sensors used in the EMVP are the following (Sanford et al., 1978):

- Two electrode assemblies (*E*1 and *E*2)
- A solenoid coil wound on a high-permeability core (*CC*)
- A bonded strain-gauge pressure transducer (*P*)
- A pressure-protected platinum resistance temperature sensor (*T*)
- An inductively coupled electrical conductivity sensor (*C*)
- A three-axis flux-gate magnetometer (*F*1, *F*2, and *F*3)
- A thermistor in the magnetometer (*TM*)
- An external thermistor (*TF*)

The major component of the profiler is the electrode and salt bridge system, which senses the microvolt potential difference across a diameter of the instrument's surface. The potential difference is the integral of potential gradients distributed on the path from one electrode along its salt bridge, around the skin through the surrounding seawater, and down the salt bridge to the other electrode. In any EM current sensor, offset voltage is an issue, and this needs to be tackled in the most optimal manner. The simplest way to make good use of the EM sensors is to protect the electrodes from environmental changes and to modulate the desired signal at a large frequency compared with the rate of electrode drift. This is achieved by the use of salt bridges, as proposed by Mangelsdorf (1962), and by the rotation of the entire instrument. Even with the use of Ag-AgCl (silver-silver chloride) electrodes, a voltage of  $\sim 350 \mu\text{V}$  will be generated for each degree in temperature difference between the electrodes of a pair.

To guard against this problem, the salt-bridge arms and electrode blocks are designed to retard heat and salt fluxes into electrodes, and the data are processed to remove the remaining slowly changing electrode offset. Taking all these into account, the electrode system (see Figure 10.18) uses large Ag-AgCl electrodes in a PVC block. The orientation of the electrode arms is determined from the signal of the compass coil (*CC*). Temperature gradients in the thermocline produce negligible errors, but bubbles in

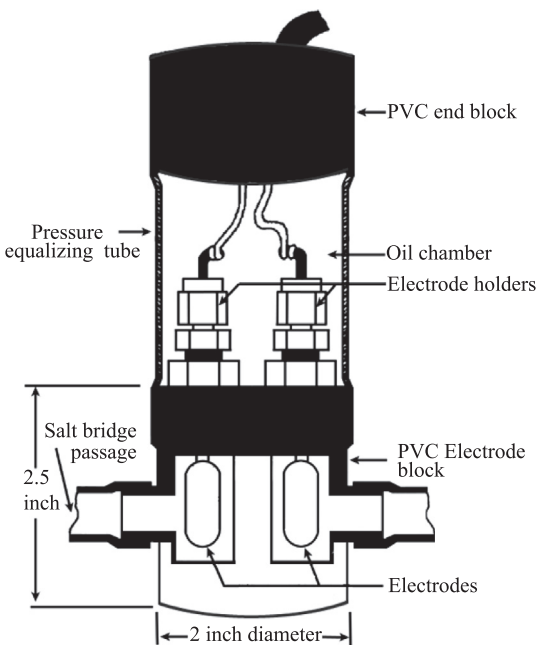


**FIGURE 10.18** Construction of electrode block of EMVP. (Source: Sanford et al., 1978.)

the tubes disturb operation within 30 m of the surface. The acoustic telemetry system provides real-time information about the current velocity and seawater temperature structure, slant range, and depth. A typical plot of the current velocity components (E-W and N-S) indicating the shear features as produced by standard processing is shown in Figure 10.19. Rapid changes of current velocity with depth in the thermocline are quite evident.

A disadvantage of the method is that it yields a profile relative to an unknown, depth-independent velocity contribution. It reveals how the ocean-flow velocity varies with depth, but the depth-averaged or barotropic component is not observed. Advantages are that the measurements are made from a self-contained, free-falling instrument. It can be used from small vessels, does not interfere with other shipboard operations, and is mobile. There are several ways by which the unknown barotropic contribution can be determined so that the velocity profiles can be made absolute. As indicated earlier, the profiler has a cylindrical form and is equipped with angled fins so as to induce steady rotation at 0.15 Hz about the vertical axis throughout its descent, thereby modulating the potential difference detected at the electrodes. This rotation enables the direction-of-flow vector to be established. It also permits the wanted signal (typically in the range 1–100  $\mu\text{V}$ ) to be extracted from much larger offset DC potentials (up to millivolts in magnitude) arising from electrochemical effects and temperature differences. A performance level of  $\pm 1 \text{ cm/s}$  at a vertical resolution of 10 m was indicated. This level is expected in the absence of

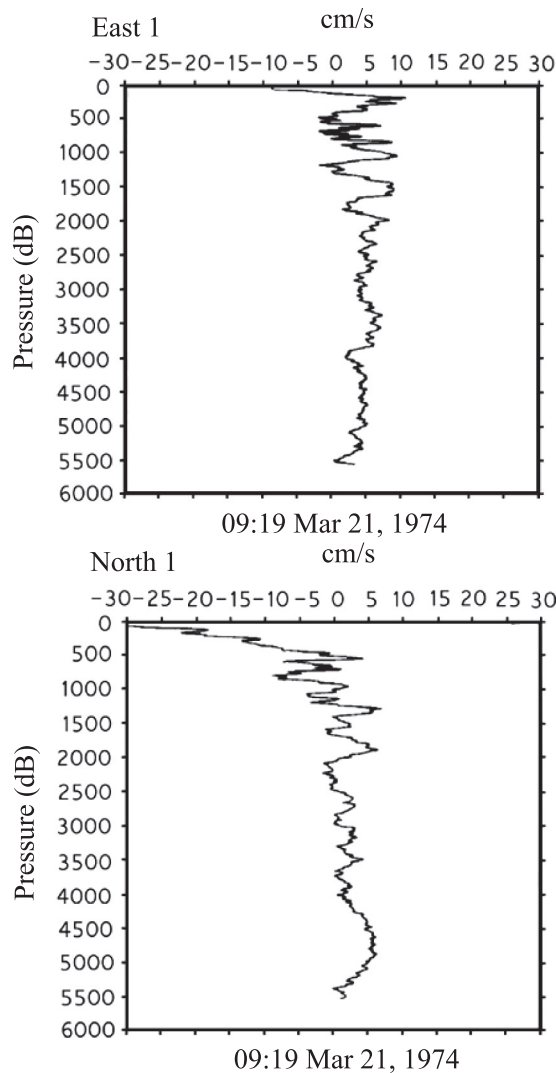


**FIGURE 10.19** A typical plot of the current-velocity components (E-W and N-S) indicating the shear features as produced by standard processing. (Source: Sanford et al., 1978.)

strong magneto-telluric currents, which can produce errors as large as 10 cm/s during infrequent (10 to 20 times per year) periods of strong temporal fluctuations of the geomagnetic field. The data (flow velocity, water temperature, electrical conductivity, pressure, and other variables) are recorded at fine temporal resolution (twice each second). The instruments have been profusely used in the western North Atlantic to describe the deep-ocean velocity profiles (Sanford, 1975); to investigate the structure and propagation of inertial period motions (Leaman and Sanford, 1975; Leaman, 1976); and to study low-frequency, baroclinic Rossby waves (Hogg, 1976).

The ocean-current profiler just mentioned and those addressed in the previous sections could not measure absolute velocity profiles; they only measured relative profiles of horizontal velocity (i.e., relative to the profiler's

velocity) as a function of depth. This is because the velocity of the profiler itself was unknown. Difficulties exist in interpreting velocity profiles from freely sinking instruments because the instrument is affected by the flow it is attempting to measure, and depending on the size, shape, and buoyancy of the probe, its trajectory may also vary from one probe to another for the same current profile. With the aid of mathematical models for the probe and from the sensor performance, the measured profile has to be interpreted as an estimate of the actual current profile (Hendricks and Rodenbusch, 1981). One method of correcting the drift-contaminated profile data would be to use commercially available acoustic positioning. This technique would, however, be tedious and restrictive in its area of operation.

The EMVP has undergone substantial refinements since its introduction, particularly in the resiting of its electrode ports for improved sensitivity. The difficulty in measuring "absolute" velocity profiles using freely falling/rising probes has been circumvented by an ingenious method reported by Sanford et al. (1985). In this modified device, known as the *absolute velocity profiler* (AVP), in addition to the relative velocity profile measured by the moving probe, an acoustic Doppler probe determines the absolute velocity of the profiler with respect to the seafloor. In construction, two acoustic transceivers on the probe, in Janus configuration, "look" toward the ocean bottom. As the probe sinks or rises, the transceivers transmit ultrasonic pings and receive the Doppler-shifted backscattered signals from the seabed. As the probe sinks toward the seafloor the returned signals are shifted "up-Doppler" in frequency, and while it rises up, the returned signals are "down-Doppler" in frequency. From measurements of the Doppler frequency shifts in the returned signals, the probe velocity relative to the fixed seafloor is independently determined. From knowledge of the acoustically measured probe velocity and the relative current-flow velocity measured by the velocity probe, the vertical profile of the absolute horizontal flow velocity is determined without depending on the hydrodynamic characteristics of the probe or additional equipment. This development thus included a measurement of  $\bar{V}^*$ . This has been achieved by mounting downward-looking Doppler sonar in the nose of the instrument (see Figure 10.20).

The transducers are arranged in a Janus configuration (see Figure 10.21). In this configuration, two transceivers of equal elevation angle point in opposite directions in the UW plane. This configuration, named after the Roman god of gates and doors who is represented as having two faces, allows determination of the vertical and horizontal components of the probe's velocity relative to the seafloor over the last 60–300 meters of the downward excursion. The advantages of the Janus arrangement are that it reduces the influences of  $W$  and small tilt errors. For a periodic

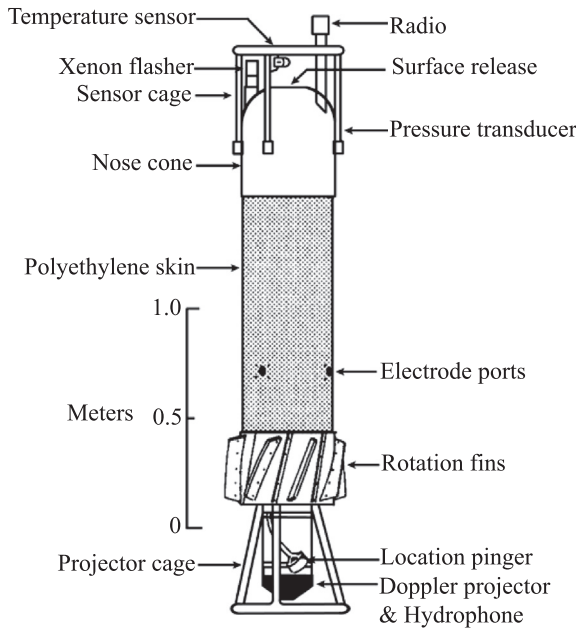


**FIGURE 10.20** Absolute velocity profiler (AVP). (Source: *Sanford et al., 1985*, ©American Meteorological Society, reprinted with permission.)

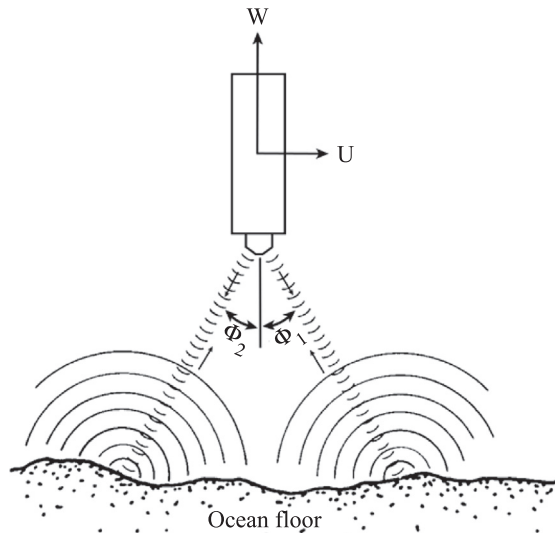


**FIGURE 10.21** AVP in which the acoustic Doppler transducers are arranged in a Janus configuration. The freely falling profiler moves with velocity components of  $U$  and  $W$  in the horizontal and vertical directions, respectively, while projecting ultrasonic beams in the directions  $\phi_1$  and  $\phi_2$  relative to the vertical. (Source: *Sanford et al., 1985* ©American Meteorological Society, reprinted with permission.)

signal transmitted and returned along a ray making the angle  $\phi$  relative to the vertical in the UW plane, the measured Doppler shift is (Berger, 1957):

$$f_{D1} = \frac{2f_1}{c}(U \sin\phi_1 - W \cos\phi_1) \quad (10.8)$$

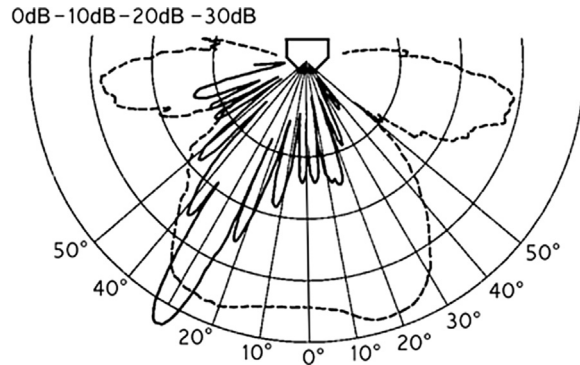


**FIGURE 10.22** Directivity patterns for the projector (solid line) and the hydrophone (dashed line) used in the AVP. (Source: *Sanford et al., 1985*, ©American Meteorological Society, reprinted with permission.)

where

$$f_{D1} = \text{Doppler frequency shift on beam 1}$$

$$f_1 = \text{transmitted frequency on beam 1}$$

$$c = \text{speed of sound in seawater at rest}$$

Given  $f_1 = 300$  kHz,  $\phi_1 = 30^\circ$ ,  $U = 10$  cm/s,  $W = -100$  cm/s, and  $c = 1.5 \times 10^5$  cm/s, estimates of the expected Doppler-frequency shifts are obtained from the previous expression as  $f_{D1} = 367$  Hz. Vehicle rotation necessitated the use of two separate frequencies for the two acoustic beams in the AVP because the narrow-beam transducers could not be used for both transmission and reception. (See the directivity patterns for the projector and the hydrophone in Figure 10.22.)

The AVP determines  $V$  at several levels, averaged over some vertical distance near the seafloor. Consequently, the combination of the acoustic Doppler (AD) and EM datasets near the seafloor yields:

$$AD - EM = V(z) - [V(z) - \bar{V}^*] = \bar{V}^* \quad (10.9)$$

Thus, subtraction of the electromagnetically derived velocities from those obtained using the Doppler sonar yields  $\bar{V}^*$ , which can then be added to the EM profile to provide the absolute current profile  $V(z)$ . Once  $\bar{V}^*$  is known, the whole EMVP profile can be adjusted so that it is an absolute velocity profile. Use of the absolute velocity profiler has shown that it can provide measurements to within 1 cm/s. A limitation of this probe, however, is that an absolute flow velocity profile can be measured only within the specified maximum slant range of the acoustic Doppler transceivers relative to the seafloor.

Electromagnetic profiling measurements clearly show promise. Duda et al. (1988) extended the technique to an autonomous instrument that can conduct multiple profiles to 1-km depth in the ocean (see Figure 10.23). Its name, *Cartesian diver*, is drawn from the toy made from an inverted bottle in which the buoyancy can be controlled by compression of an enclosed volume of gas while it is

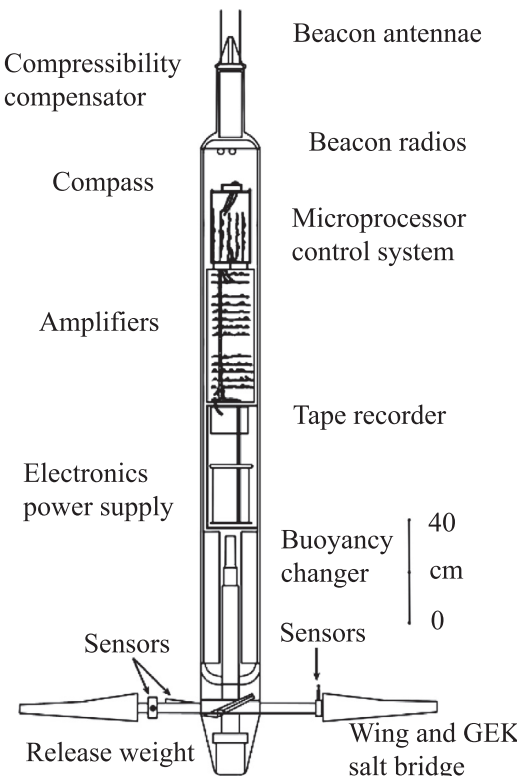


**FIGURE 10.23** Side view of the Cartesian diver profiler. (Source: Duda et al., 1988, ©American Meteorological Society, reprinted with permission.)

submerged in a liquid. The device was used prior to Descartes to illustrate the incompressibility of water relative to air, but Descartes' name has since been associated with it. The oceanic Cartesian diver has been engineered primarily to record continuous profiles of horizontal velocity using a variation of the method of geomagnetic induction, such as those reported by Sanford et al. (1978) and Sanford et al. (1982).

The assumption made in the estimation of the horizontal velocity of the diver is that the ocean electric field  $E_s$ , measured in a stationary coordinate system, does not vary with depth. Consequently, the electric field measured in the reference frame of a drifter,  $E' = E_s + V \times B$ , yields the drifter velocity  $V$ . Here  $B$  is the local magnetic induction. The diver records the horizontal components of the apparent electric field, which includes the effect of all three components of the diver's velocity. If the instrument moves horizontally at the same speed as the surrounding fluid and if its vertical velocity is steady or known, then vertical shear of horizontal velocity is directly determined from the vertical variations of the measured horizontal electric field.

The vertical velocity of the water is estimated by observing the vertical velocity of the instrument relative to the surface with a pressure gauge. Because the package profiles at terminal velocity, changes in its falling or rising

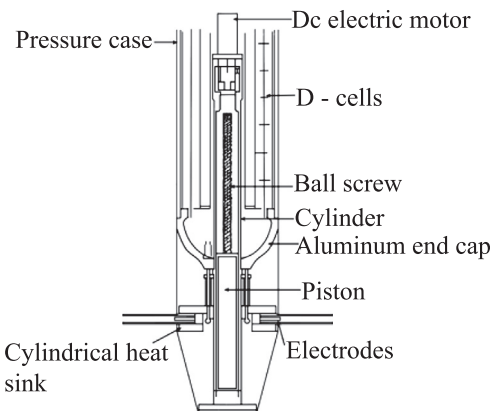


**FIGURE 10.24** Cross-section of the Cartesian diver profiler showing the electrodes within two salt bridges within the disk-like heat sink. The ball-screw-driven volume-changer piston is shown in extended position. (Source: Duda et al., 1988, ©American Meteorological Society, reprinted with permission.)

rate can be attributed to the vertical motion of the surrounding fluid.

The *Cartesian diver* is an untethered autonomous device that alternately falls and rises freely through multiple cycles, recording data internally. The diver propels itself vertically by adjusting its volume while its mass is unchanged, thereby changing its buoyancy. The instrument rotates once in 3 m vertically.

One feature of untethered profilers is that they have constant and reproducible dynamics. Because they fall and rise at a characteristic terminal velocity, the force required to propel them is equal to the drag at that velocity. Buoyancy of the diver is changed by moving a piston, which seals a cylinder extending through the bottom end cap. The recovery release assembly is attached to the lower end of the cylinder, which is open to seawater. Because the density of seawater changes rapidly through the thermocline and the instrument is virtually incompressible, a passive compensation piston at the top end of the diver is used to give the entire instrument roughly the same compressibility as seawater as both seawater temperature and pressure vary in that region. Without the compensation, the Cartesian diver would fall at an ever-decreasing rate throughout its descent and would rise at an increasing rate. The diver is equipped with beacon radios and a programmable underwater acoustic transponder to facilitate recovery.

The diver's buoyancy change is implemented by a ball-screw-driven volume-changer piston at the lower end of the diver (see Figure 10.24). The piston is sealed with a sealing ring. A DC electric motor with a reduction gear drives the piston through a ball-screw jack. A servo-controlled electromechanical brake must be energized to physically release the motor for motion. Both the motor and brake voltage regulators are of the switching type in order to

conserve battery energy. The buoyancy changer is controlled by an onboard computer, and the decision making can be based on any measured parameter such as seawater pressure, temperature, or time. The buoyancy is always changed to its maximum or minimum value so that the instrument can only rise or fall at its maximum speed. The logic behind this choice is that to simplify statistical analysis of repetitive profiles, it is desirable for the Cartesian diver to move at a constant vertical velocity.

The buoyant forces that propel the instrument are determined by the difference in density between the instrument and the water surrounding it. Density adjustments are made with the buoyancy changer only as the instrument changes direction, but during the course of a profile the density difference between the instrument and the seawater must remain constant. The density of seawater increases more rapidly with pressure than that of the aluminum pressure case. To compensate for this, a highly compressible volume of gas is added to the instrument to make its overall compressibility more similar to that of seawater. The gas volume is in the form of a cylinder sealed with a piston. One side of the piston is exposed to ambient pressure. The piston is captured when the gas has expanded to a predetermined level. The O-ring seal of the two-piece, hollow piston is lubricated with oil forced out from within the piston. The gas volume is pressurized with a regulated gas bottle before the instrument is launched.

Silver-silver chloride electrodes with 5–25 cm<sup>2</sup> of exposed silver are used to sense the induced voltages. They provide a stable, low-noise electrical connection to the surrounding seawater. Unfortunately, the noise spectrum of the measurement electrodes is quite similar in shape and magnitude to the signal spectrum that would be sensed if the profiler simply profiled and recorded the potentials due to its horizontal drift, without spinning. The electrodes also have a thermal coefficient, which will create error voltages if the electrodes change temperature relative to one another or if that coefficient varies between members of an electrode pair. To record the induced voltage signal despite the red noise and to achieve 5-m resolution of water-current velocity, the electrodes must be physically interchanged at 0.03 Hz or faster in as short a vertical distance as possible (i.e., at a high wave number). This is a modulation of the signal spectrum into the frequency (wave number) of rotation. Higher modulation frequency and higher modulation wave number each give smaller effective rms noise velocity and better resolution of the water-current velocity. The interchange of the electrodes is accomplished by spinning the instrument with four wings, which have a span of 1.60 m. Adjustment of the wings allows profiling velocity variation over a range  $\pm 20$  percent of the nominal velocity. Having two pairs of electrodes provides redundancy and a method for evaluating electrode noise levels.

The wings are made of epoxy-Fiberglas skin over polyethylene pipe. The foil sections are symmetrical in order to have the same lift and drag characteristics for both rising and falling motions. To minimize the voltages induced by temperature differences and to provide insulation from the changing temperature of the passing seawater, the electrodes are mounted within a 0.05-m-tall, 0.11-m-diameter cylindrical heat sink made of aluminum and PVC. The electrical conducting paths from the ocean to the electrodes extend through the polyethylene wing pipes, filled with agar and seawater, which serve as salt bridges. The resistance of each salt bridge is about 500 ohms, contributing insignificant thermal agitation noise of 3 nV rms in each of the two voltage channels over the 0.25 Hz bandwidth of the instrument. The lattices of agar suppress noise by preventing water of varying conductivity from flowing into and out of the salt bridges. The salt bridges extend the effective electrode positions away from the pressure case. Effective 1.6-m electrode separation, rather than the 0.22-m case diameter, provides voltage gain and allows a measurement of the motionally induced voltage uninfluenced by the presence of the instrument body (Sanford et al., 1978). Thus the Cartesian diver differs from the geomagnetic inductive profilers of Sanford et al. (1978) and those of Sanford et al. (1982) by measuring the electric field away from the body of the instrument instead of one perturbed by the presence of the instrument.

With the end assemblies in place and with an expendable ballast “drop weight” attached at the lower end, the instrument has a total length of about 3 m and a total mass of 90 kg. The drop weight is released by venting a vacuum chamber that holds on the weight. The venting is performed at a prearranged time by two redundant explosive devices activated by countdown timers. At this time, profiling is suspended and the instrument floats to the surface, extending two beacon radio antennae well out of the water.

The Cartesian diver is a quasi-Lagrangian drifter in the horizontal in the sense that it moves with the mean velocity of the water through which it profiles. Because it profiles through a sheared horizontal velocity field, it cannot follow the water at any depth in a horizontally Lagrangian manner, even if instantaneously perfectly Lagrangian in the horizontal. The Lagrangian character distinguishes the diver from moored instruments, past which there is continual advection, and from instruments that profile from a ship moving through the water. One appropriate use for the diver is study of the evolution of properties of water mass. Another is the determination of statistical differences between separate water masses, such as variations of the internal wave field on either side of a front (Duda and Cox, 1987).

The Cartesian diver, which is an untethered and unguided, axially spinning and horizontally drifting, self-profiling device that has the capability to alternately fall

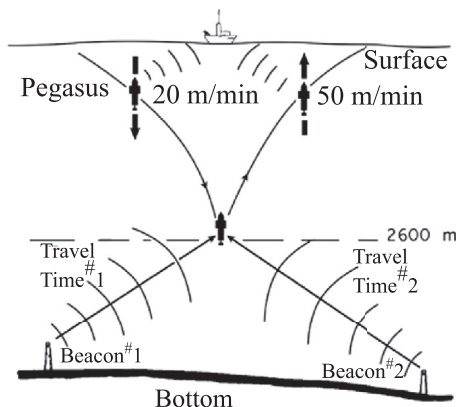


**FIGURE 10.25** Schematic diagram showing acoustic tracking of free-falling current velocity profiler (Pegasus) relative to two expendable beacons. (Source: Spain et al., 1981.)

and rise freely through multiple cycles at almost equal down- and up-characteristic terminal velocity, is perhaps a marvel in the realm of electromechanical engineering design in the field of oceanography. The ability to make Lagrangian measurements is an important feature of this diver-probe. However, this very feature also renders it unsuitable to make repeated vertical profiling in a given location of interest.

### 10.2.6. Free-Falling, Acoustically Tracked Absolute Velocity Profiler (Pegasus)

As noted in Section 10.2.3, measurement of absolute ocean-current velocity profiles by the method of acoustic tracking of a free-falling pinger was first introduced by Rossby (1969). In this method, the differences in the time of arrival of an individual acoustic pulse at four or more hydrophones were measured. Hyperbolic tracking was then used to fix the position of the pinger, and the trajectory was differentiated to compute the current velocity profile. The hardware positioning was later reversed (Pochapsky and Malone, 1972) so that acoustic transponders were bottom-mounted and the hydrophone was contained within a free-falling float. The acoustic travel times from the sources to the receiver, as well as water pressure and temperature at the hydrophone, were telemetered to a support vessel. When travel times were measured, the spherical tracking method (as opposed to the hyperbolic tracking method used by Rossby, 1969) could be used to compute the trajectory of the moving hydrophone. In later instruments (Luyten and Swallow, 1976), the free-falling hydrophone was used as self-recording probe for monitoring travel times, water pressure, temperature, and salinity in the close vicinity of the probe.

Spain et al. (1981) reported a free-falling current velocity profiler, which is acoustically tracked relative to two expendable beacons (see Figure 10.25). In this scheme,

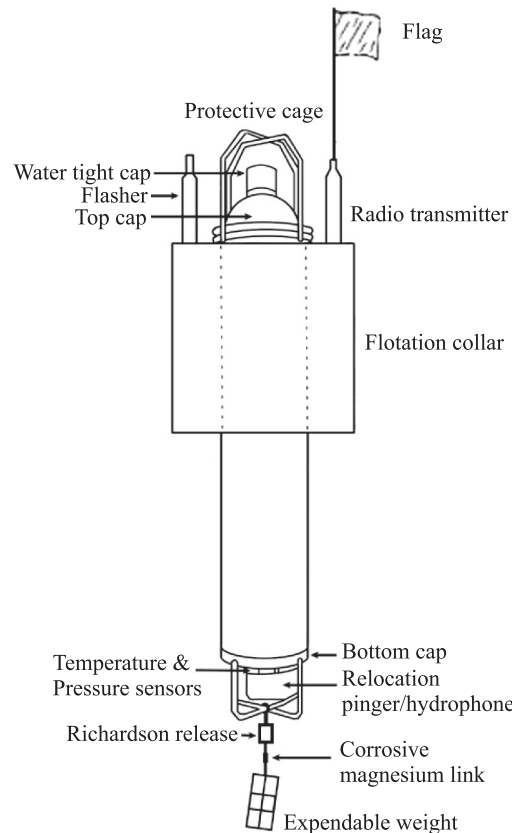


**FIGURE 10.26** Free-falling ocean current velocity profiler (Pegasus). (Source: Spain et al., 1981.)

regular acoustic transmissions from the profiler enable its movement to be monitored from a ship. Every 8 seconds, water pressure (depth) and temperature, together with the two travel times from the beacons, are logged in the profiler Pegasus (see Figure 10.26). The profiler sinks at a speed that enables the fine structure in the vertical to be resolved accurately.

Pegasus is a compact and lightweight probe. The pressure case is an 80-cm length of 6061-T6 aluminum tubing with an outer diameter of 17.5 cm and wall thickness of 1.25 cm. A hemispherical top cap is permanently fixed to the tube, whereas the flat bottom cap is removable. The tube and end caps can nominally withstand a pressure equivalent to 3,000-m seawater depth. A syntactic foam floatation collar is fastened to the outside of the pressure case to provide 10 kg of positive buoyancy. Two pitched fins are fixed on opposite sides of the collar. As the profiler descends and ascends, the fins cause it to rotate, thereby removing any effects of an asymmetric weight distribution on the profiler's motion.

Standard recovery aids such as flag, radio, and flasher are inserted into the top of the collar. Cages are attached at either end of the probe to protect the sensors and watertight seals. A recovery line is tied to the top cage, and

a Richardson hydrostatic weight release (Richardson and Schmitz, 1965) is secured to the lower cage. Pegasus weighs 45 kg in air. Four kilograms of expendable weight sink the profiler at a constant vertical velocity of 20 m/min and the expendable weight is dropped at a preselected depth by the Richardson release. A corrosive link is the backup weight release. The recovery aids and 5 cm of the floatation collar are visible when the instrument is floating at the surface.

In Pegasus, all the sensors are mounted on the bottom end cap. Whereas water temperature, pressure, and oxygen probes penetrate the end cap, the acoustic transducer is simply mounted to it. The acoustic transducer includes a diode transmit-receive switch that allows the transducer to serve as both the relocation pinger and the hydrophone. An 8-ms acoustic pulse is transmitted every 8 seconds at 10 kHz so that the movement of the profiler can be monitored from the ship. These transmissions can also be used for the interrogation pulses for transponders. During the remaining time, the transducer is used as a hydrophone across the 11- to 13-kHz band. The low-level input from the hydrophone is fed to a preamplifier, which also band-pass-filters the signal between 11 and 13 kHz. The signal is then sent to three signal detector circuits, each of which is centered on a specific beacon frequency. The detectors band-pass-filter the signal in a wide and narrow band. When a signal is received from a given beacon, the rms level in the relevant narrow band rises much more than in the corresponding wide band. If the ratio of the rms levels in the two bands exceeds a threshold for a duration of 4 ms, a beacon signal is considered to have been received. An output pulse is sent to the stop gate of the corresponding travel-time counter. Water temperature is measured by a thermistor with an accuracy of 0.03°C. A strain-gauge pressure transducer with a nominal accuracy of 0.5 percent makes pressure measurements. The oxygen sensor (optional) measures the dissolved oxygen in water. The acoustic travel times and the profiler-borne sensor outputs are logged in the memory bank of the profiler. At a typical descent speed of 20 m/min, the profiler will complete a 2,500-m cast in 3 hours.

The expendable beacons used with Pegasus are constructed from a 30-cm length of 7075-T6 aluminum tubing with an outer diameter of 12.5 cm. The beacons weigh 6 kg and are sealed by two 2-cm-thick flat end caps. A transducer with an acoustic output power of 91 dB re 1  $\mu$ bar at 1 m is mounted to the top cap of the beacon. With this power, the beacon signals can be heard at distances in excess of 7 km. At a profiling site, two of the three operational frequencies (11.5, 12.0, and 12.5 kHz) are used; the third is available for a backup beacon. The beacons, sealed by evacuation, can nominally withstand a pressure equivalent to 5,500-m seawater depth.

The beacons are deployed while the ship is underway at a constant speed and heading so that a reasonable estimate

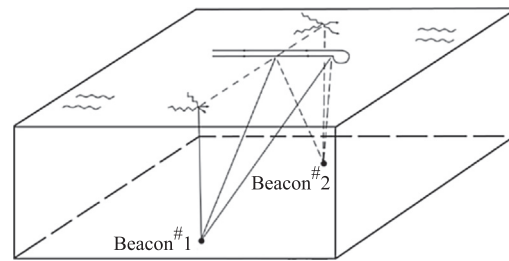


**FIGURE 10.27** Beacon survey method. (Source: Spain et al., 1981.)

of their juxtaposition can be made. More accurate measurements of the separation distance and orientation are made in a survey of the beacons. The acoustic travel times from the beacons are continuously monitored on a graphic recorder. In the survey, the ship makes several passes at each beacon to try to pass directly overhead. During a pass, the ship is continuously maneuvered to minimize the travel time from the beacon to the ship. When the ship passes directly over each beacon, a minimum acoustic travel time is recorded. After the beacon depths have been ascertained, the ship steams steadily on a heading to intersect the baseline perpendicularly. When the baseline is crossed, the minimum travel times for that heading are measured (see Figure 10.27). Using Pythagorean geometry, the baseline length is determined from the minimum slant ranges and beacon depth measurements. A reciprocal heading is sailed to make a second crossing of the baseline. The ship's velocity on each heading is computed in both the geographical and beacon reference frames. Vector subtraction of these velocities removes the effect of the ocean currents and enables the baseline direction to be ascertained. The just-mentioned technique does not depend on electronic navigational aids.

When the beacons are deployed, they ping synchronously with each other, with Pegasus, and with a timing reference aboard the ship. However, if a profiling site is later revisited, any drift in the transmission time of the beacons must be determined before absolute travel times can be recorded. To determine this drift, the ship must travel directly over each beacon, and a minimum acoustic travel time must be measured relative to the timing reference, as indicated earlier. Because the travel time corresponding to the water depth is already known, the transmission time of each of the beacons relative to the reference can be computed. Pegasus's timing must also be similarly referenced so that the offset between the clocks in the beacons and the profiler can be measured.

Spain et al. (1981) reported the profile data collected by Pegasus. In their measurements, a constant descent rate was assumed for Pegasus. This approach correctly resolved the fine structure. When Pegasus was tracked, the measured water pressure determined its vertical position. Its horizontal position was fixed by the two slant ranges to the

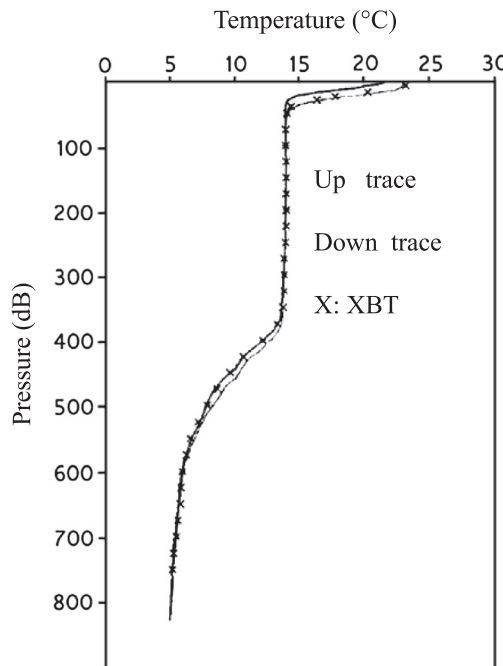


**FIGURE 10.28** Water-temperature profiles measured by Pegasus. (Source: Spain et al., 1981.)

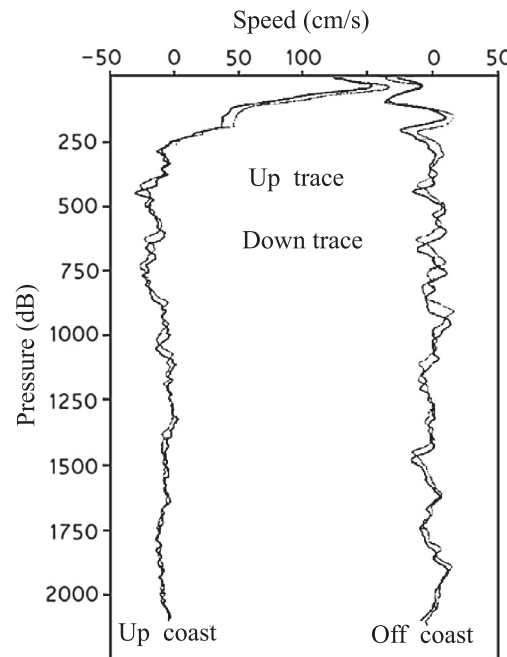


**FIGURE 10.29** Water-current profiles measured by Pegasus. (Source: Spain et al., 1981.)

beacons. Errors in current velocity profile measurements come from various sources such as depth error, baseline length error, and refraction effects of the sound rays in the ocean environment. These aspects have been analyzed in great detail by Spain et al. (1981). After poor position fixes had been discarded by a simple running filter, horizontal water-current velocities were determined from the trajectory and volume transports were calculated by integrating the velocities. Figures 10.28 and 10.29 show temperature and water-current profiles, respectively, measured by Pegasus.

A glass-housed version of Pegasus was reported by Cole (1981). This modified version incorporates a number of advantages over earlier versions in aluminum housings. These advantages include operation to full ocean depth, integral floatation, no corrosion, optical synchronization where desirable, and large battery capacity. The enhanced battery power supply allows 100 deployments without opening; a very ample safety factor for a normal cruise is usually about 20 deployments. As in the case of the aluminum units, the glass units are also small, easy to handle, and easily shipped. Enhancement was also achieved in the bottom-mounted acoustic array and the shipboard data handling and storage unit. The electronics of Pegasus consist of two subsystems: (1) a data collection unit, which measures water pressure and temperature and up to three acoustic travel times; and (2) a microprocessor-controlled data storage package, which also controls the operation of the Pegasus instrument itself.

The acoustic tracking system used with the modified Pegasus instrument has the feature of either bottom transponders or beacons. Both methods have been used successfully. When a bottom array of free-running beacons is used, precise synchronization of the beacons and the Pegasus instrument clocks is required. Because of the glass housing, this synchronization can be carried out without opening the housing. The Pegasus instrument acoustic transmitter (in the transpond mode) and receiver (both modes) are based on a novel approach (Hayward and Ferris, 1979) that provides extremely low jitter, thereby giving good resolution and accuracy of position. It is of great value to be able to preview the data immediately on return of the instrument without opening it. A simple software package has been developed to present the data in graphic form so that the success or failure of a particular deployment can be assessed immediately before moving to the next station.

### 10.2.7. Freely Falling, Acoustically Self-Positioning Dropsonde (White Horse)

Luyten et al. (1982) have reported a dropsonde system known as *White Horse*, which was designed and constructed at the Woods Hole Oceanographic Institution by W. J. Schmitz, Jr., and R. Koehler and first deployed in 1972 (Gould et al., 1974) to determine vertical profiles of horizontal velocity. This device is a freely falling instrument package that interrogates bottom-moored acoustic transponders (see Figure 10.30) and records internally the

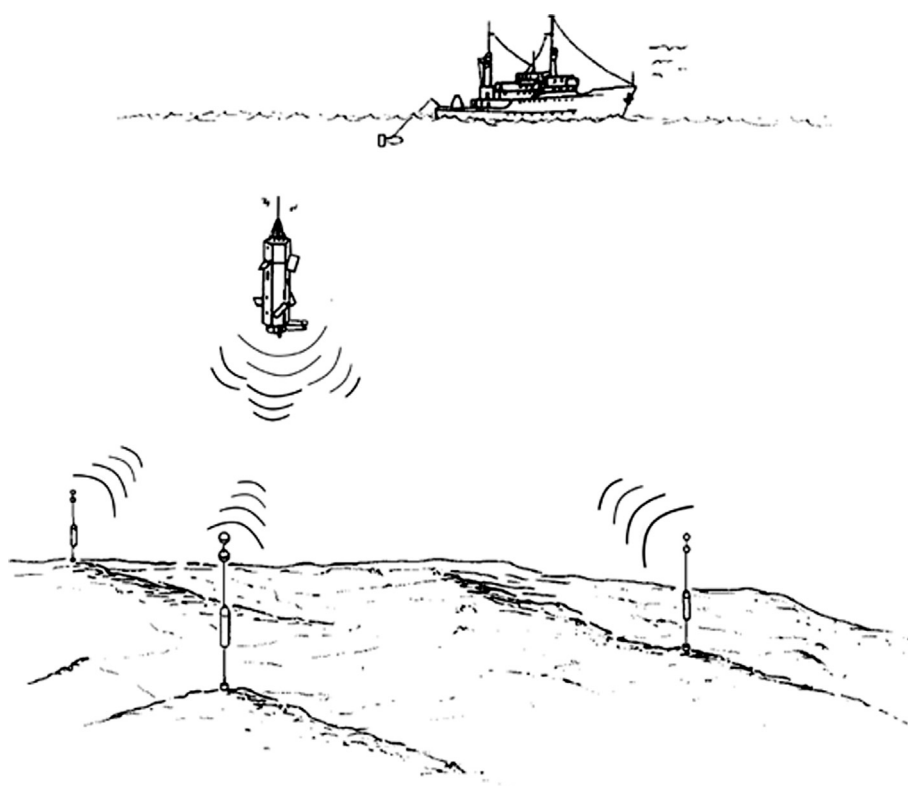


**FIGURE 10.30** Diagram showing the freely moving instrument package known as White Horse, which interrogates three bottom-moored acoustic transponders. (Source: *Luyten et al., 1982.*)

time elapsed between the interrogation and reply pulses. The interrogation cycle is initiated every 20 s. The White Horse system also includes a Neil Brown microprofiling CTD operated at 1 Hz. The instrument is ballasted to fall and rise at approximately 1 m/s. The acoustic navigation package was designed around an underwater navigation package marketed by EG&G Sea Link using its transponding releases. It is a four-channel system in which the instrument transmits a 20-ms pulse at 11 kHz and the bottom-moored transponders reply at 9.0, 9.5, and 10.5 kHz. The fourth channel provides a spare in case one of the other channels becomes unusable. (Standard use of four transponders provides redundant navigational data.) When the instrument detects a reply pulse in one of the receivers, the appropriate time-interval counter is stopped. The time intervals are stored in a shift register, which is transferred onto the Sea Data cassette when the next interrogation pulse is transmitted. The CTD samples data (16 bits) once in a second. At a fall or rise rate of 1 m/s, this corresponds to a nominal 1-m vertical resolution for the CTD. Data are logged on the cassette every second.

The dropsonde is ballasted to descend to the ocean floor, where it can be released by any of three independent release mechanisms: an acoustic release, a preset timed release controlled by the internal master clock, or a corrodible link. The former two methods have been found to be very reliable.

The White Horse consists of four instrument packages: (1) the navigator-controller, (2) CTD, (3) an acoustic release, and (4) a data recorder. Each unit is contained in a standard 5-in. ID anodized aluminum deep-sea pressure case. The cases are cable-connected and placed in the vehicle, constructed of rigid plastic with syntactic foam for buoyancy. There is sufficient reserve buoyancy for the instrument to remain slightly buoyant if all the pressure cases become flooded. The assembled vehicle (see Figure 10.31) has a hexagonal cross-section of  $0.7 \text{ m}^2$ , an

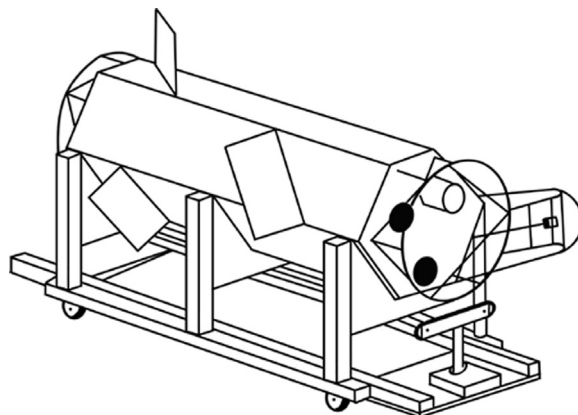


**FIGURE 10.31** Drawing of White Horse, depicting its hexagonal cross-section of  $0.7 \text{ m}^2$  and an overall length of 1.75 m. (Source: *Luyten et al., 1982.*)

overall length of 1.75 m, and a mass of 475 kg. To increase the stability and avoid erratic skating motions, fins have been added to make the instrument rotate clockwise as it falls at approximately one revolution per instrument length.

To record a profile at a given site, three acoustic transponders are deployed in a triangular array on the seafloor and surveyed before the dropsonde probe is deployed. This generally requires 4–5 hours if a towed fish is used for the survey. The dimensions of the triangular array must be comparable with the ocean depth. Although a longer baseline array reduces the navigation errors somewhat, the S/N ratio is also reduced due to longer acoustic paths, and consequently more data are lost. The transponders are tethered approximately 20 m above the ocean floor, resulting in some mooring motion, normally 10 to 15 cm, but there is less chance of the refracted acoustic rays intersecting the ocean floor.

The relative coordinates of the transponder array are determined by interrogating the array from the sea surface. The White Horse system is used for such interrogations with a transducer suspended 15 m below the freely drifting ship. To reduce errors in the determination of the coordinates of the transponder array, a pattern of 13 interrogation sites is used. These sites are equally spaced around the perimeter of a triangle, which is twice the size of the transponder net. An additional site is chosen in the center of the net. The orientation of the transponder net relative to North can be determined by using absolute navigation fixes, together with simultaneous acoustic ranges. The dropsonde is deployed from the ship's crane near the center of the transponder net. The dropsonde descends to the seabed and is released after a few minutes on the bottom, either acoustically or with a timed release.

The slant range between the dropsonde and the ship is monitored using a deck clock, which is synchronized with the instrument to drive a precision graphic recorder. Because the ascent rate of the dropsonde is nearly constant and the time of anchor release from the bottom is known, the slant range can be converted to an approximate horizontal range from the ship to the instrument. With this information it is possible to be near the instrument when it surfaces (typically 200 m). A submersible radio and light are used as recovery aids and are particularly useful if acoustic contact with the instrument is lost.

As in the case of any freely falling/rising probe, the profile of local horizontal current velocity in the ocean is estimated from the horizontal displacement of the White Horse relative to the bottom-moored transponders. Systematic and random errors affect the accuracy of the current velocity estimates. The errors are those associated with the acoustic navigation of the instrument and those involved with the interpretation of the horizontal velocity of the instrument as oceanic motion. The latter are

generally hydrodynamic in origin. The individual sources of error in position and velocity determination are given in Luyten et al. (1982). Despite various sources of error, intercomparison measurements against a vector-averaging current meter (VACM) have indicated that the average difference between the White Horse and the VACM measurements are 0.5–0.7 cm/s, with standard deviations (2.0, 1.6) cm/s for the (east, north) components. Although no direct simultaneous comparisons have been made between the White Horse and other similar profiling instruments, Rossby and Sanford (1976) reported comparisons between the EMVP and an acoustic dropsonde similar to the White Horse. They concluded that the observed differences between the EMVP and the acoustic dropsonde are not significantly different from the expected errors in each technique. Evans and Leaman (1978) reported further comparisons between the White Horse and the University of Miami PCM. The differences between the two sets of observations were reported to be within the margins of errors appropriate for the two systems. Detailed assessments of the observed errors in the vertical profile of horizontal currents have indicated the importance of using the correct local sound-velocity profile (a climatological average may suffice in some circumstances) for the current profile and survey calculations. The key to the success of the dropsonde technique is considered to be matching the accuracy of the navigational technique to the particular environment. For the pulsed acoustic navigation system, the dominant error arises from uncertainties in determining the leading edge of the acoustic pulse. As with any dropsonde technique used in the measurement of the vertical profile of horizontal currents, the accuracy is related to the vertical resolution by an uncertainty principle  $\Delta u \Delta z = w \Delta x$ , where  $\Delta u$  and  $\Delta z$  represent the average horizontal velocity error (due to position errors) and sampling depth interval, respectively. In this expression,  $w$  and  $\Delta x$  represent the vertical motion speed (i.e., fall rate) of the profiler and the error in the horizontal position of the profiler, respectively. It has been found that using the system in the White Horse, current-velocity profiles can be determined with an accuracy of  $\pm 4$  cm/s over 25-m depth intervals.

### 10.2.8. Freely Rising Acoustically Tracked Expendable Probes (Popups)

A limitation of the acoustic dropsonde methods discussed in the previous sections was that the spatial separations of the transponder array needed to be comparable with the ocean depth. Accurate determination of the coordinates of the transponders was also difficult. Furthermore, even the bottom-moored transponders needed to be tethered approximately 20 m above the ocean floor in order to avoid the refracted acoustic rays intersecting the ocean floor

(Luyten et al., 1982). This resulted in some motion of the transponders, causing errors in the estimation of the vertical profiles of the horizontal current flow velocities.

These limitations have been circumvented in a design reported by Voorhis and Bradley (1984). This device is a self-contained, bottom-mounted instrument for measuring vertical profiles of horizontal current in the deep ocean over long time periods (up to a year). It employs an interferometric technique to track small, expendable, buoyant probes containing CW acoustic beacons, which are released on a preset schedule. A carrying capacity of 60 probes is feasible. Tracking data are stored in the bottom instrument and retrieved after recovery. The overall profiler system consists of an open pyramidal frame with a triangular base (5 m on each side) outfitted with a canister of simple, expendable, buoyant acoustic probes and three tracking hydrophones located at the three corners of the pyramid base (Figure 10.32).

The pyramidal frame is constructed with aluminum tubing that can be unbolted easily to permit air shipment and field assembly. Beneath the main frame is a releasable anchor frame that supports the entire unit on the seafloor and remains on the bottom when the unit is recovered. Recovery buoyancy is provided by nine glass floatation spheres attached to the sides of the main frame. The complete instrument, including anchor frame (250 kg), weighs about 570 kg in air and 114 kg in water. Without the anchor frame, the instrument has a positive buoyancy of  $\sim 120$  kg.

The three tracking hydrophones are mounted rigidly on the outer corners of the main frame base, allowing an undisturbed acoustic “view” of the ascending probe. The receiving hydrophones are identical to the probe transmitter

element and are a piezoelectric crystal type contained in oil-filled boots. The three bottom hydrophones receive a continuous incoming signal from the rising monochromatic probe, which transmits a 15-kHz CW tone with an acoustic wavelength of 10 cm. Each hydrophone has a preamplifier with band-pass filtering at  $15 \pm 2$  kHz. The hydrophones are directional and reject acoustic radiation from below.

The primary electronics, which include a complete recovery command system, tracking receivers, data logger, internal magnetic compass, and instrument tilt sensor, are contained in a single pressure case suspended vertically from the apex of the main frame. Mounted on top of the main pressure case are the instrument recovery beacon and a command receiver/transducer. Thus, all components associated with recovery are part of this single pressure housing. Additionally, the release mechanism is a shared double release that can be activated by a command, either to the main command receiver/transducer or, as a backup, to a completely independent release in a second tube that is mounted alongside the main electronic housing.

The distance from the ascending probe to each hydrophone is determined by measuring and keeping track of the phase difference between a fixed, precision frequency source within the bottom unit and each incoming signal from the ascending probe, the frequency of which has been Doppler downshifted by the probe’s upward motion. Signal processing required to achieve better precision in distance measurement is accomplished as follows: The electrical signal from each hydrophone goes to a superheterodyne receiver with a noise bandwidth of approximately 10 Hz. In this receiver, the hydrophone signal is multiplied by a constant 15.1515 kHz signal, giving sum and difference frequencies, termed by Voorhis and Bradley (1984) as *interferometric technique*. A narrow-band phase-lock loop tracks the difference frequency of  $\sim 151$  Hz and multiplies it by 512. This  $\sim 77$  kHz signal goes to a free running counter, the contents of which are recorded at each sampling interval. The least-phase count is therefore equivalent to an acoustic phase resolution of  $2\pi/512 = 1.2 \times 10^{-2}$  rad at each hydrophone. Thus, the signal phase is measured with a resolution of 1/512 cycle so that in the absence of significant noise, the slant range to the probe is measured with a resolution of  $\lambda/512$ . This scheme made it possible to have a much shorter baseline compared to the pulse system, where the baseline needs to be comparable to the ocean depth. The advantage of using phase-lock loops is that it permits the tracker to “flywheel” over occasional dropouts in the acoustic signal if they occur.

The launch of Popup is shown in Figure 10.33. A schematic of the expendable acoustic probe assembly (Hoyt, 1982) is shown in Figure 10.34. The expendable probe is constructed from thick-walled cylinders (7.5 cm outer diameter, 2.5 cm inner diameter) of high-density

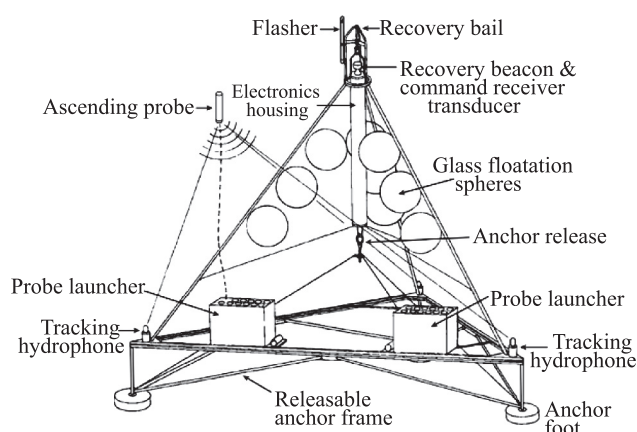


**FIGURE 10.32** The Popup profiler system consisting of an open pyramidal frame with a triangular base (5 m on each side) outfitted with a canister of simple expendable buoyant acoustic probes and three tracking hydrophones located at the three corners of the pyramid base. (Source: Voorhis and Bradley, 1984, ©American Meteorological Society, reprinted with permission.)

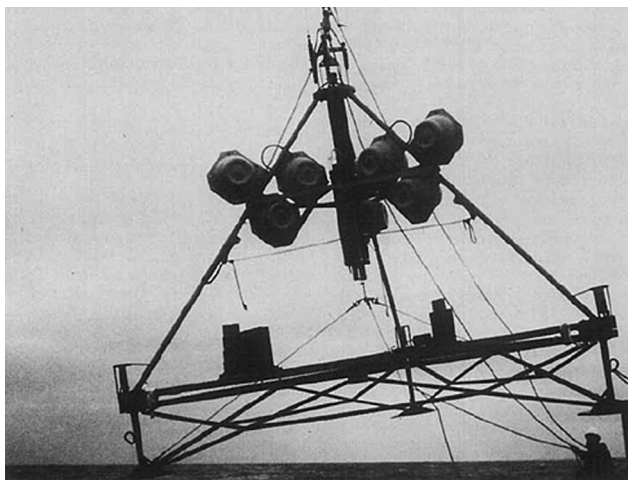


**FIGURE 10.33** Launch of Popup. (Source: Voorhis and Bradley, 1984, ©American Meteorological Society, reprinted with permission.)

syntactic foam ( $0.6 \text{ gm/cm}^3$ ) enclosed by syntactic foam end caps. The overall height of a probe is 47 cm, and it ascends to the sea surface in a vertical orientation. Within the central cavity are the battery pack (four alkaline C cells) and electronics. The latter consist of a 15-kHz crystal-controlled oscillator, amplifier, and matching transformer to drive the acoustic transducer, which is mounted in an oil-filled boot on the bottom of the probe. The drive circuit

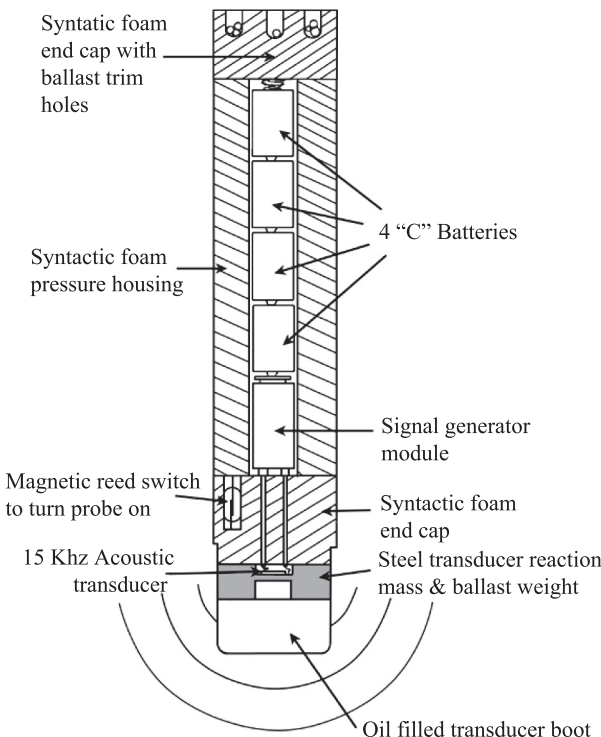


**FIGURE 10.34** Schematic of the expendable acoustic probe assembly. (Source: Voorhis and Bradley, 1984, ©American Meteorological Society, reprinted with permission.)

automatically shuts down after 5 or 10 hours to prevent interference with subsequent probes. The transducer is a piezoelectric crystal type tuned to 15 kHz. A heavy metal disk sandwiched between the lower end cap and the acoustic transducer serves the following purposes (Voorhis and Bradley, 1984):

- Increasing the probe weight to near-neutral buoyancy in seawater
- Lowering the center of gravity and increasing vertical stability
- Improving the acoustic radiation pattern (i.e., decreasing the ratio of upward to downward radiated power); this minimizes phase interference from surface reflection as the probe approaches the sea surface

Syntactic foam construction suffers from two limitations: (1) relatively low compressive strength, which must be compensated for by the thick wall construction of the probes, and (2) buoyancy loss due to water absorption over long periods at high pressures.

The probe begins its ascent at the preset time after a warm-up period of 30 min, during which the receivers in the main housing lock on and the probe frequency stabilizes. A reasonable ascent rate for the probes is 25 cm/s so that 5–6 hours are required to reach the surface.

The bearing of the rising probe with respect to the bottom unit is calculated from the difference in slant ranges to the three hydrophones. The trajectory of the ascending probe is measured and recorded within the bottom unit. The bottom unit is recovered at the end of the deployment mission and the probe trajectories analyzed. Successive determinations of positions of the probe are used to estimate the oceanic current field. Figure 10.35 shows east and north components of trajectory and horizontal velocity of the probe released on May 28, 1983, at  $39^{\circ}00'N$ ,  $69^{\circ}00'W$ . Probe ascent speed was 35 cm/s and water depth was 3,110 m. Data were sampled every 2 s, smoothed by an 80-s triangular window and plotted every 40 s (14-m depth intervals).

It may be noted that no field measurements are free from errors. The probe just described also suffers from such limitations. Tracking error is one such error. This arises from random variations in acoustic phase and hence in the measured travel times to the probe. Although the probe is designed for downward radiation of acoustic signal, some degree of upward radiation is also present. Such radiations from the ascending probe get reflected from the sea surface and are added to the direct downward radiated signal, producing a phase uncertainty at the hydrophones. This uncertainty is small when the beacon is deep, because of the large distance to the surface and back (spherical spreading). The uncertainty becomes significant, however, as the probe nears the surface, where it becomes the major source of random error in the Popup tracking system. The phase

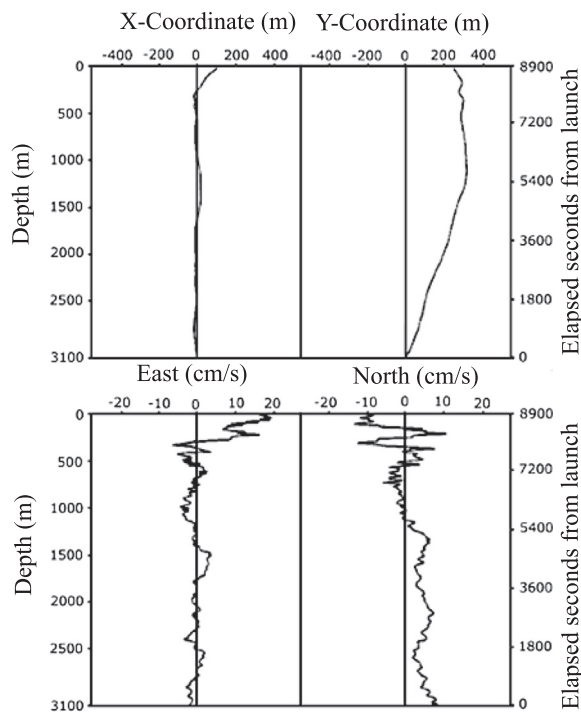


**FIGURE 10.35** East and north components of trajectory and horizontal velocity of the probe released on May 28, 1983, at  $39^{\circ}00'N$ ,  $69^{\circ}00'W$ . (Source: Voorhis and Bradley, 1984, ©American Meteorological Society, reprinted with permission.)

uncertainty depends on the acoustic directivity of the probe (upward to downward radiated power). Voorhis and Bradley (1984) found that digital processing of the acoustic phase data with a triangular weighting filter over 80 s reduces the near-surface probe position error to about 70 cm and horizontal current velocity errors to about 2 cm/s for a 14-m vertical resolution. They also noticed occasional large phase fluctuations that cause probe tracking to jump one or more phase “lanes” (i.e., change by multiples of  $2\pi$  radians), particularly when the probe was near (or on) the sea surface. However, because the phase jumps must be exactly an integer number of cycles, it was possible to add or subtract the missing cycles to generate a continuous trajectory. This strategy can be successful only if the phase lock loops are out of lock a small fraction of the time.

Apart from the previously mentioned problem, another issue that may deteriorate the performance of the tracking system is the changes in the probe signal frequency during its ascent, primarily due to thermal drift of the resonant frequency of the crystal oscillator in the beacon as it ascends into warmer layers of the upper ocean. Yet another aspect that might deteriorate the measurement accuracy is the uncertainty in converting the travel time to slant range. The conversion requires knowledge of the nonfluctuating sound velocity along the acoustic ray paths, including the effects of refraction, from probe to hydrophones. However,

in the absence of sound-velocity measurements by the probe, errors arising from poor knowledge of sound velocity profile can be ameliorated by acquiring it independently, either from hydrographic measurements at the site or from historical data appropriate to the site.

An improved design that does not require an array of bottom-moored transponders is a phased-array hydrophone and an expendable, free-falling, and depth-measuring pinger, reported by Riggs et al. (1989). In this method the pinger’s slant range, depth, and azimuth relative to a single hydrophone deployed below the sea surface from a vessel are determined at regular time intervals throughout the descent. A crystal-controlled clock in the shipboard electronics is synchronized with a similar clock in the probe prior to the deployment. The probe’s range is then obtained from a synchronized pulse, which is transmitted by the probe. As the slant range of the probe to the hydrophone increases, the time delay of the incoming signals relative to time of synchronization is measured and the range calculated. The probe depth relative to the sea surface is determined by a pressure transducer, which is housed in the base of the probe, and the depth data are transmitted to the surface. The angle of arrival of the incoming signal is measured by the hydrophone’s ultra-short-baseline phased array. The measurement of changes in the phase of the incoming signals as they pass over the elements of the array allows for an accurate determination of the azimuth. Once the three-dimensional trajectory of the probe is determined, the speed and direction of horizontal flows at various depths are estimated from the predicted dynamic response of the probe relating its horizontal displacement and the oceanic current velocity. Comparative statistics indicated (Riggs et al., 1989) that such a probe can measure speed and direction of horizontal flows accurate to better than  $\pm 4$  cm/s and  $\pm 10^{\circ}$ , respectively, for current speeds of 30 cm/s or greater.

### 10.3. TECHNOLOGIES USED FOR VERTICAL PROFILE MEASUREMENTS OF OCEANIC CURRENT SHEAR AND FINE STRUCTURE

It was found to be difficult to measure the detailed velocity structure of important western boundary currents, such as the Kuroshio and the Gulf Stream, by means of conventional moored current meters, primarily because of the motion of mooring lines due to strong currents and the deployment cost of a mooring system over a wide area. In view of such difficulties, freely dropped ocean current profilers were developed (Halkin and Rossby, 1985; Leaman et al., 1987) for the study of vertical fine-structure regimes ( $1m < \lambda < 100m$ ). Subsequent research in this area gave rise to the development of more advanced technologies. These are addressed in the following sections.

### 10.3.1. Free-Fall Shear Profiler (Yvette)

The first requirement for an instrument intended to resolve small-scale ocean-current velocity and shear is that its own motion be quiet so that it can fall freely through the water column rather than be cable-lowered from a ship. Second, both the water-current velocity and water-density sensors must have fine resolution, because it is necessary to detect differences in these properties over small vertical scales. Third, the velocity and density measurements should be made simultaneously, at the same point in space. To fulfill these requirements, [Evans et al. \(1979\)](#) reported the design of a free-fall instrument, known as Yvette, which simultaneously resolves the local current velocity field relative to the instrument as well as the density field. Yvette was designed primarily to investigate the relations between shear and density gradient on small scales.

The Yvette comprises a 4-m, ~17-cm circular long tube (which provides the basic framework and flotation), the lower end of which houses a current meter and sensors for measurements of water conductivity, temperature, and pressure (CTD). The electronics main frame and batteries are all located at the lower end to give the instrument vertical stability against shear-induced tilting (see [Figure 10.36](#)). A protective cage surrounds the sensors and supports the pressure-actuated ballast-release systems. At the upper end of the tube is a 10-kHz pinger with 4-s repetition rate, flasher, and radio as well as all aids required for relocation and recovery. The current-sensing device used in this profiler is an ATT difference current meter developed by Trygve Gytre at the Christian Michelsen Institute of Bergen, Norway. In the present application, the CM sensor design sought a compromise between the need to obtain a good S/N ratio and the need to keep the acoustic transducers as small as possible, to avoid disturbance to the current flow, and their separation large enough to obtain a high acoustic pulse travel-time difference value. The compromise was to choose the probe

distance about twice the diameter of the pressure housing. With this arrangement and careful electronic design, the current meter is capable of measuring correctly both static and dynamic currents from ~1 mm/s to ~1 m/s.

A master clock in the profiler controls the entire operation at a basic sampling rate of 2.5 Hz. A problem that seems to characterize long tubes such as this is a tendency for them to behave like pendulums. The Yvette exhibits a small-amplitude oscillation with a period of ~5 s. By working backward from a worst-case current-velocity measurement, where the 5-s oscillation had an amplitude of 0.25 cm/s, the amplitude of the oscillation was estimated to be less than 0.02°. Such oscillation was found to introduce a resonant peak in the shear data. Vortex-shedding surfaces of the profiler were found to be responsible in part for exciting these oscillations and could be attenuated by reducing such surfaces. The observed resonant peak in the shear data could be removed using a digital notch filter. The Yvette rotates slowly while sinking, and its body motion effectively high-pass-filters the velocity profile to scales smaller than the rotation scale.

Yvette was subjected to comparison studies by attaching a pinger to it, and a number of profiles were made in the U.S. Navy underwater tracking range at St Croix, U.S. Virgin Islands. [Figure 10.37](#) shows a comparison of two components of velocity obtained by differentiating the tracking data (tracked) and reconstructing the profile from Yvette (computed). The overall agreement on scales up to about 100 m is good, with the difference less than  $\pm 3$  cm/s. [Figure 10.38](#) shows two components of vertical shear from St Croix tracking range data. It has been found that Yvette can resolve the high wave-number end of the internal wave band and the transition region to smaller three-dimensionally turbulent scales. The instrument has been deployed for study of the relation between mesoscale features and small-scale mixing.

### 10.3.2. Acoustically Tracked Free-Fall Current Velocity and CTD Profiler (TOPS)

As mentioned earlier, the dropsonde proved to be a convenient tool for vertical profiling of horizontal ocean currents. However, in situations in which one's interest is in the study of vertical fine-structure regimes ( $1\text{m} < \lambda < 100\text{m}$ ), the translation of the dropsonde itself must be adequately accounted for because at long vertical wavelengths, the dropsonde nearly follows the fluid motion and the measured relative velocity is small. In addition, the profiler body often has a natural oscillation frequency, which, at reasonable fall rates, induces spurious current velocity measurements in the fine-structure region.

Thus, to understand the relative velocity measurements, it is necessary to model the response of the dropsonde to the imposed shear flow. The actual ocean current velocity is

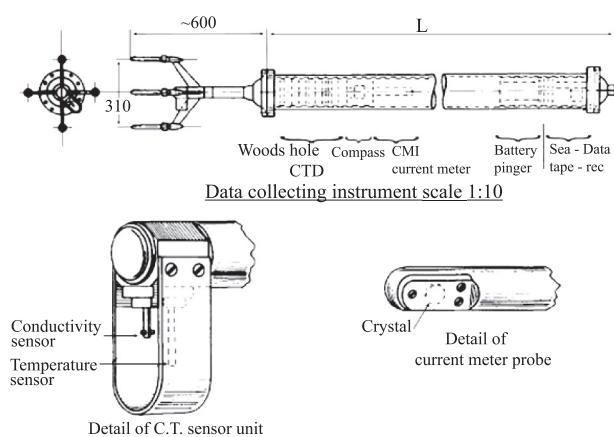


**FIGURE 10.36** Diagram of Yvette. (Source: [Evans et al., 1979](#).)

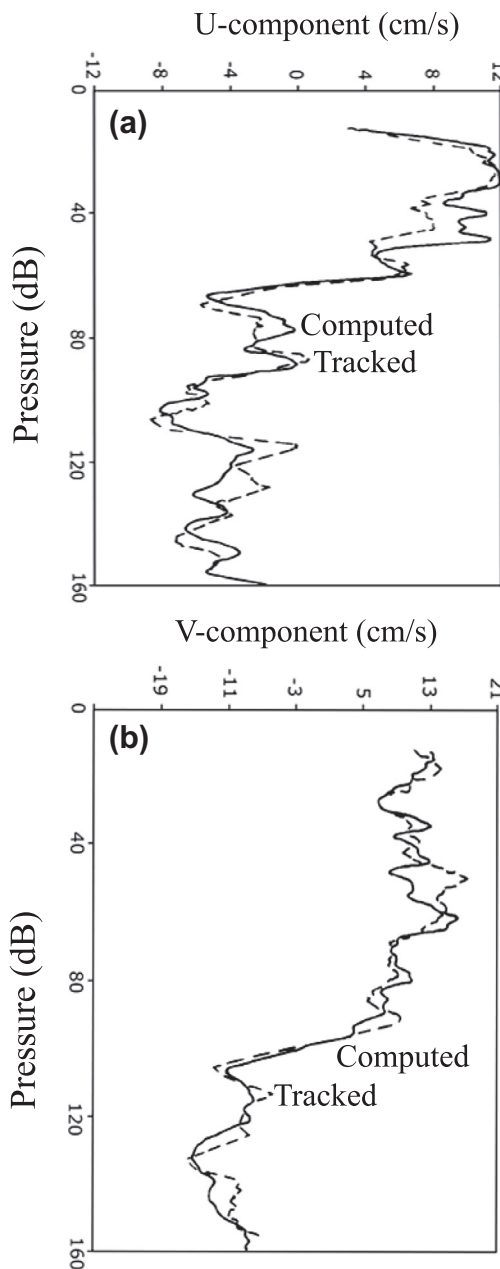


**FIGURE 10.37** (a) East-west and (b) north-south components of current measured from St Croix, U.S. Virgin Islands, by the inversion routine (computed) and by acoustic tracking with bottom-mounted hydrophones. An arbitrary zero offset has been added to the computed values because Yvette makes only a relative measurement. (Source: *Evans et al.*, 1979.)

then extracted by a transfer function acting on the measured velocity. Limitations on this velocity computation occur at long wavelengths because of sensor drift and at short wavelengths because of sensor size and sensitivity. Techniques that measure ocean-current velocity by tracking a freely falling body's trajectory relative to some fixed coordinate system are the natural complement to onboard CM measurements. Deriving ocean-current velocity from

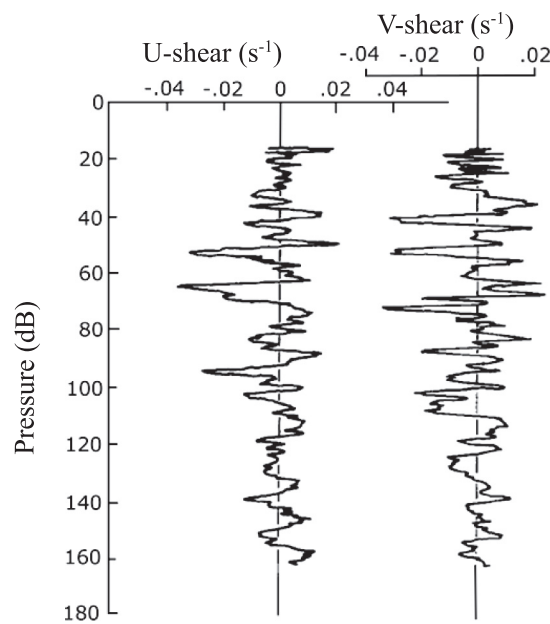


**FIGURE 10.38** Two components of vertical shear from St. Croix tracking range data. (Source: *Evans et al.*, 1979.)

the trajectory of a freely falling body requires that the body be in equilibrium with the current flow in the vicinity. Thus, this technique well resolves the long vertical wavelength structure but smoothes the small-scale fluctuations. However, simultaneously tracking a dropsonde with an onboard current meter yields a profiler capable of resolving vertical scales from the fine-structure range up to the total water depth. Hayes et al. (1984) reported one such instrument, named TOPS (Figure 10.39). In this case, relative velocity measurements are provided by an onboard two-axis acoustic current meter, and the trajectory of the free-fall profiler is measured by acoustically tracking it relative to an array of bottom-moored transponders. Whereas estimation of vertical profiles of horizontal flow velocity using a simple acoustic dropsonde depends entirely on its trajectory, the acoustic CM incorporated into the free-fall instrument, TOPS, measures ocean-current velocity relative to the profiler. In other words, the CM measures the relative velocity between the dropsonde and the surrounding water masses at various depths. Motions of the profiler are monitored with a two-axis accelerometer and flux-gate compass. TOPS' profiling capability extends throughout the full water column (6,000-db pressure limitation). The relative velocity measured by the CM provides additional data to the estimates of the vertical profiles of horizontal flow velocities. From the trajectory described by the dropsonde as well as the relative velocity measured by the CM, the absolute flow velocities at various depths are inferred using an appropriate hydrodynamic model, resolving velocity fluctuations that have vertical wavelengths as small as 0.2 m. Additional

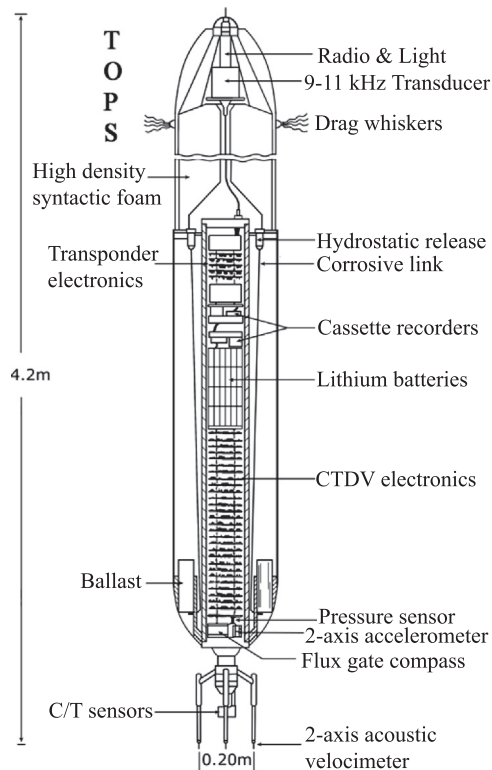


**FIGURE 10.39** Schematic drawing of TOPS. The lower portion contains the onboard sensors: two-axis acoustic current meter, flux-gate compass, CTD and two-axis accelerometer. The upper portion contains the acoustic tracking system. (Source: Hayes et al., 1984, ©American Meteorological Society, reprinted with permission.)

parameters measured by TOPS are water conductivity and temperature.

The acoustic tracking system associated with TOPS is similar to that described by Luyten et al. (1982). In operation, an array of three bottom-moored acoustic transponders is deployed. The relative location of the array elements is determined by a ship survey. During profiling, TOPS is dropped near the center of the net. If for some depths or at some locations, replies from only two bottom transponders are available, then the trajectory and velocity of the TOPS are estimated from these replies, combined with the measured pressure from the CTD. Because TOPS usually rotates slowly (1 revolution per 100 m) about its axis of symmetry, the compass goes through several oscillations. Plotting the  $x$  and  $y$  components against each other should describe a circle. If necessary, the components are adjusted in offset and amplitude to yield a circle centered on zero.

As TOPS falls through the ocean, it is subjected to a variety of forces that result from the relative velocity between the vehicle and the water. Consequently, interpretation of the TOPS onboard velocity measurements requires a model that describes the response of the profiler to the ocean shear flow. If motions of the vehicle can be

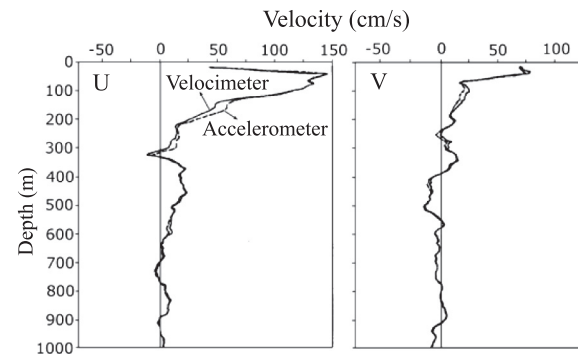


**FIGURE 10.40** Ocean-current velocity profiles obtained by inverting the TOPS model using relative velocity measured by the acoustic current meter (solid) and those estimated from the measured acceleration (dashed). In the latter case, the low-frequency form of the transfer function was used. (Source: Hayes et al., 1984, ©American Meteorological Society, reprinted with permission.)

accurately predicted given only the relative water velocity at the nose (which is measured), it is possible to infer the actual water velocity by combining vehicle and relative velocities. In practice, there is always an arbitrary constant velocity that cannot be obtained solely from the relative velocity measurement. However, this barotropic component is measured by the acoustically tracked velocity profile.

Models of the response of freely falling long cylindrical profilers (similar to TOPS) to shear flows have been discussed in several studies, but none of them account adequately for the distribution of forces along the body or the inclination of the body relative to the vertical. To account for these effects, Hayes et al. (1984) developed a two-dimensional model for TOPS. Figure 10.40 shows ocean-current velocity profiles obtained by inverting the TOPS model using relative velocity measured by the acoustic current meter and those estimated from the measured acceleration. Measurements have shown that TOPS and the dynamic model that describes its motion are efficient tools that permit study of the vertical structure of oceanic velocities over vertical wavelengths from 0.20 m to the total water depth. This spectrum encompasses the mesoscale and fine-structure regimes. The principal components are the combination of acoustic tracking and onboard CM measurements (both of which had been used independently in several previous instruments) and a linear model that permits reconstruction of current velocities through the fine structure region where vehicle motions potentially contaminate ocean-current velocity estimates. In addition, the full-depth capabilities of the instrument permit study of fine-structure velocities in the weakly stratified abyssal ocean. These measurements have provided new insights into the relationships between large and small vertical-scale ocean currents and the underlying physical processes.

## 10.4. TECHNOLOGIES USED FOR VERTICAL PROFILE MEASUREMENTS OF OCEANIC CURRENT SHEAR AND MICROSTRUCTURE

Several types of free-fall instrument packages that provide vertical profiles of horizontal currents have been addressed in the previous sections of this chapter. Apart from such measurements, oceanographers have shown keen interest in examining the vertical microstructure (i.e., wavelengths  $\lambda$ , shorter than 1 m), where the major concern is shear over vertical length scales that are much less than the instrument length. At such scales, only the high-frequency vibrations of the profiler affect the measurements; the lateral translation of the body can be neglected. Technologies used for vertical profile measurements of oceanic current microstructure are addressed in the following sections.

### 10.4.1. Towed Acoustic Transducer

Probably the first experiment conducted to examine the feasibility of measuring ocean-current shear is the one reported by Thomas (1971) using acoustic backscattering. Measurements of reverberation statistics carried out by Thomas with a towed transducer indicated that volume backscattering can be used to measure ocean-current shears over the interval occupied by deep scattering layers—normally from near the surface down to depths of 400 to 1,000 m. A series of experiments performed by Thomas employed an acoustic transducer towed behind a ship and with a searchlight beam pattern, as indicated by the broken line in Figure 10.41. An impeller speedometer attached to the towed body gave a continuous record of the transducer speed relative to the water with an accuracy of about 0.1 knot. Tone pulses of temporal width  $\tau = 0.5\text{--}1\text{ s}$  and 9.5-kHz frequency were transmitted, and the backscattered acoustic energy was received by the same transducer. Velocity of sound profile and corresponding ray plots of acoustic propagation indicated downward refraction of acoustic energy through the deep scattering layers (see Figure 10.42). The rays correspond to energy leaving the transducer horizontally and at  $\pm 5^\circ$ . Downward refraction eliminates surface backscattering at distances beyond 0.4 km.

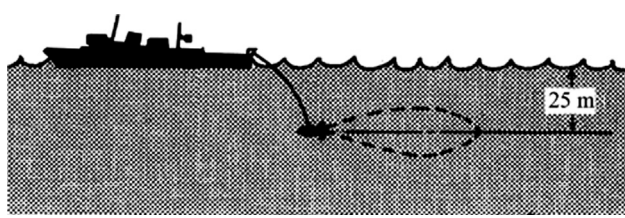


**FIGURE 10.41** Schematic diagram depicting the use of an acoustic transducer towed behind a ship for measurement of the vertical profile of ocean-current shear. (Source: Thomas, 1971.)

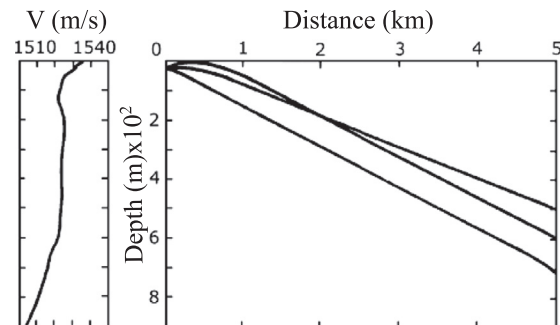


**FIGURE 10.42** Examples of velocity of sound profile (left) and ray plots showing acoustic energy refracted downward through the deep scattering layers (right). (Source: Thomas, 1971.)

In several of the experiments, conditions were such that the reverberation was entirely due to volume scatterers beyond some relatively short distance where the surface was no longer insonified. Most of the volume backscattering in deep-water areas is from relatively small organisms that are presumably carried along by the water current. If water current is primarily in a horizontal direction, one might expect the current shear structure to remain much the same over relatively large areas in the deep ocean. Downward refraction of the acoustic energy means that the received volume backscattering corresponding to increasing time steps (i.e., from increasing radial distances) arrive from increasing scatterer depths. The relative velocity between the acoustic transducer and the moving scatterers give rise to Doppler shift in the received acoustic energy. Thus, the frequency spectrum of reverberation at any time after transmission, corresponding to some distance interval, gives the effective radial velocity distribution of the scatterers over the water volume insonified at that distance and depth.

Figure 10.43 indicates that the average frequency or Doppler shift of the reverberation changes with distance due to changing radial velocity components of the scatterers. Thus, spectra of successive samples of reverberation of the form shown in Figure 10.43 enable estimation of the horizontal current velocity vectors as a function of depth. All that is required are the mean reverberation Dopplers (ensemble averages of from 30 to 50 samples of spectra in order to obtain statistically significant estimates), the transducer headings (preferably  $90^\circ$  apart), and the calculated angles from the horizontal at which acoustic energy reaches the scatterers at different depths. During periods of vertical migration of scatterers, which usually occur near sunset and sunrise, some errors could exist in measurements, depending on the rate of migration and the percentage of the relevant scatterers migrating.

Although the transducer used in Thomas's (1971) experiments was not optimum for current shear measurements, the results obtained were sufficient to demonstrate

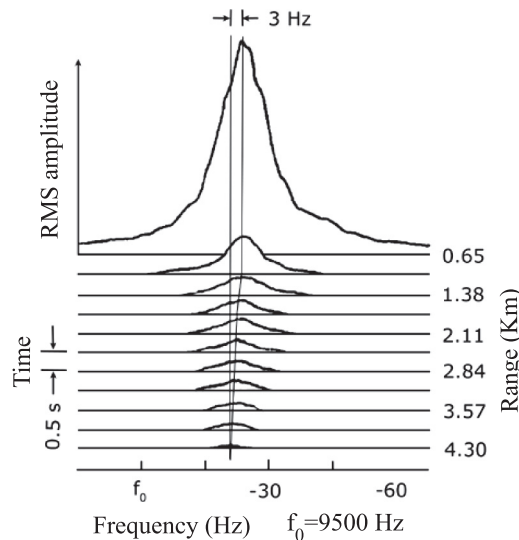


**FIGURE 10.43** Root mean power spectra of reverberation at half-second time intervals corresponding to successive scattering volumes separated by 380 m. The average frequency or Doppler shift of the reverberation changes with distance due to changing radial velocity components of the scatterers. (Source: Thomas, 1971.)

the effect of horizontal current shears. Better measurements should be possible using transducers with narrower stabilized vertical beams and higher acoustic frequencies whereby pulse lengths could be shortened.

The technique Thomas (1971) used is a valuable tool for both continuous monitoring and sampling of ocean-shear currents. The transducer could be mounted on the seafloor or, with suitable stabilization, on a buoy, in a towed body, or on a ship's hull. Perhaps the greatest attraction is that, combined with velocity of sound measurements using expendable bathythermographic equipment, this acoustic technique could provide relatively quick sampling of near-surface ocean-shear currents without lowering complex equipment through the water column.

#### 10.4.2. Free-Fall Probe (PROTAS)

Knowledge of small-scale flow-velocity structure in the ocean is meager in relation to what is known of the density structure. Techniques for the observation of temperature and salinity (and therefore density) in the ocean are well established and have been widely exploited. For instance, Woods (1969a) described a probe measuring the temperature difference over a vertical spatial interval of 10 cm, which falls down a vertical wire, and observations on vertical scales of less than 10 cm have been reported by several other researchers. This method overcomes the difficulties associated with vertical and horizontal ship motions transmitted to conventional TSD systems by the supporting cable.

Often, the water-flow velocity gradient in the ocean is concentrated into the regions of intense water-density

gradients. For closely examining such velocity gradients, it is helpful to have an instrument that is capable of resolving velocity differences as small as 1 mm/s over vertical separations down to ~30 cm. Because of the generally small velocity changes observed in the deep oceans, even weak coupling to ship motions would be unacceptable; therefore, a completely free-fall system was considered imperative. Such a free-fall system makes only relative velocity measurements unless it can be provided with a reference frame by, for example, an acoustic navigation system—a requirement that would severely restrict observations. A technique for establishing a reference frame has been described by Plaisted and Richardson (1970), who used a conventional current meter lowered at a slow uniform rate from a free-floating spar buoy. To obtain an absolute velocity profile, the CM velocities were combined with the velocity of the spar, which was determined by repeated plotting on Hifix.

An ingenious method of measuring velocity shear developed by Drever and Sanford (1970) made use of the electrical currents that flow in response to water movement in the Earth's magnetic field. The method is not absolute, however, but determines the horizontal velocity, with a vertical resolution of 8 m, relative to its value averaged over the entire depth.

A further difficulty arises from the small magnitude of the velocity differences to be detected. Even in a relatively high-shear region such as the seasonal thermocline, Woods (1969b) found from observations of dye tracers that the largest shear corresponds to a change of velocity of ~1 cm/s in an interval of 10 cm. His results suggested that useful observations should be able to resolve velocity to ~1 mm/s at speeds of 1 cm/s or less, a requirement that cannot be met by any of the conventional instrumentation used in oceanography.

Simpson (1972) reported a probe for measuring small, vertical scale variations in the horizontal velocity field. This probe, named Probe Recording Ocean Temperature and Shear (PROTAS), designed and constructed at the National Institute of Oceanography in the United Kingdom, was intended to overcome the problem of measuring small flow-velocity changes by the use of a neutrally buoyant vane. In this system, the vane is attached by a low-friction universal joint to a framework that protrudes from the main body of the probe (see Figure 10.44). As well as being neutrally buoyant, the vane is ballasted so that there is no static moment about its center of gravity. Consequently, the attitude of the vane is controlled entirely by the dynamic forces associated with the flow past it. The vane responds to changes in the horizontal velocity in a distance approximately equal to its own length of 30 cm.

In contrast, the body of the probe, which consists of a long circular cylinder, is subject to a large static righting moment of ~6 N m per degree of deflection from the

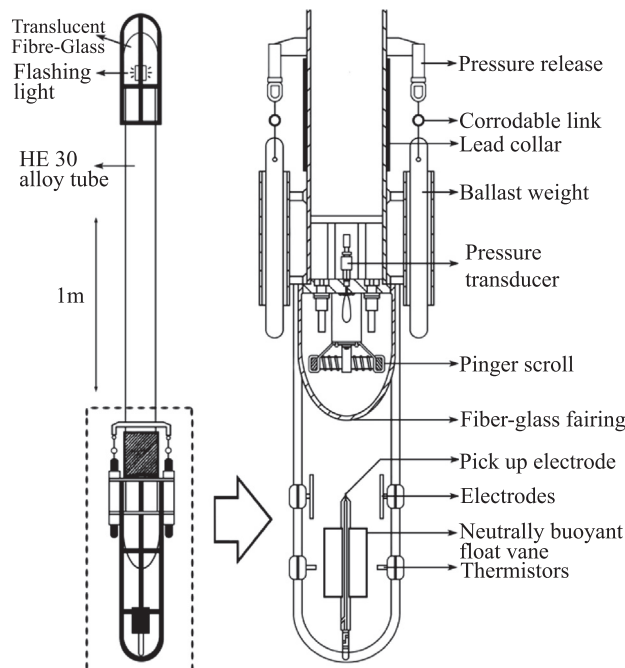


**FIGURE 10.44** Construction of PROTAS and details of the sensing head. (Source: Simpson, 1972.)

vertical. It falls at between 20 and 40 cm/s under a net weight of  $\sim 100$  gwt. Under the action of the largest dynamic moment envisaged, it deflects less than  $0.1^\circ$  from its equilibrium position. Deflection of the vane relative to the vertical defined by the probe is therefore an indicator of any horizontal velocity difference between the probe and the water.

Any change in horizontal velocity encountered by the probe in its descent will cause a displacement of the vane. It will also cause the body to experience a horizontal acceleration, with the result that the observed velocity shear will differ from its absolute value. If  $u$  and  $v$  are the absolute horizontal velocity components and  $u'$  and  $v'$  the values relative to the probe, this may be expressed as (Simpson, 1972):

$$\frac{du}{dz} = \frac{du'}{dz} + \frac{\dot{p}}{W} \quad (10.10)$$

$$\frac{dv}{dz} = \frac{dv'}{dz} + \frac{\dot{q}}{W} \quad (10.11)$$

In these equations,  $\dot{p}$  and  $\dot{q}$  are the components of horizontal acceleration and  $W$  is the free-fall vertical velocity. By making  $W$  large, the correction term can apparently be suppressed. Unfortunately, this is not the case in practical terms, because  $\dot{p}$  and  $\dot{q}$  both are dependent on  $W$ , increasing almost in proportion to it.

In addition, because the vane displacement sensitivity is inversely proportional to  $W$ , making  $W$  large does not make

sense. In practice, the correction term is found to be small and its value may be estimated from the known relative velocity profile. To do this, the flow past the cylinder is considered an axial flow with an independent two-dimensional cross-flow. It was found that if the length of the body can be made to exceed the dominant vertical length scale of the velocity structure, the accelerations  $\dot{p}$  and  $\dot{q}$  would be reduced. This observation suggests that the cylindrical body of the probe must be as long as is practical. In computing the acceleration of the probe, it is assumed implicitly that the probe is not rotating or at least that it does not rotate significantly in its own length. This assumption about PROTAS was found to be reasonably valid in field trials at sea in which it was fitted with a recording compass. The rate of rotation was then found to be  $\sim 1$  revolution per 100 meters of depth.

Movement of the shear-detecting vane is sensed by an electrode on the end of the vane, which picks up two alternating voltages provided by pairs of fixed electrodes. The pick-up electrode is, in effect, the wiper of two resistive potentiometers formed by the pairs of fixed electrodes. The two signals are at different frequencies and can, therefore, be separated by tuned amplifiers and converted by phase-sensitive detection to voltages that, for small displacements, represent the rectangular coordinates of the tip of the vane. At a fall speed of 30 cm/s and with a vane of 30-cm length, a cross-flow of 1 mm/s produces a vane movement of 1 mm, which is a displacement readily detectable by the pick-up circuitry.

Justifying the name of the probe (i.e., Probe Recording Ocean Temperature And Shear), the PROTAS incorporated a fast-response temperature gradient measurement as well so that velocity and density gradients may be compared in fresh water. Since it is a profiler, its depth measurements are also made. Temperature and depth measurements are made by conventional thermistor and strain-gauge techniques and simultaneously recorded. The thermistor is a Fenwal GB32, which has a time constant of  $\tau \sim 150$  ms and hence a vertical resolution of  $\sim 5$  cm for  $W = 30$  cm/s. A still faster response thermistor GC32 ( $\tau = 80$  ms when mounted in a pressure-proof unit) will allow a slight improvement on the vertical resolution.

The temperature gradient is estimated by differentiating the output from a single thermistor. In freefall, where the vertical velocity  $W$  is accurately known, the time rate of change of temperature may be interpreted as a spatial gradient. To improve the S/N ratio, the conventional active differentiator circuit is preceded by a low-noise amplifier.

In construction, the body of the probe consists of an HE 30 WP alloy tube of wall thickness 6.35 mm and diameter 18 cm, which can operate to a depth of 500 m with a safety factor of 2. Adequately thicker-walled tubes that can overcome collapse due to elastic instability and yielding of the metal will be capable of reaching the deepest oceanic

depths. The ends of the tube are streamlined by Fiberglas fairings, which also house the recovery aids. At the lower end of the tube there is a 10-kHz acoustic beacon; in the upper fairing, a discharge tube flashing light is provided to assist in locating the probe at night. The righting moment is further enhanced by the positioning of the ballast weight and the lead collar, which is used for ballast adjustments. To achieve the necessary degree of static stability, the internal payload (electronics, batteries, and recorder) is carried in the lower half of the tube. When the probe reaches its terminal depth, the ballast is released by one of the two tension-pin pressure releases. The second weight is detached by a corrodible link, which also acts as a back-up time release in the event of a failure in the hydrostatic system.

The first successful trials of the prototype system were made in 1970 from a research vessel in Loch Ness in Scotland, which is a freshwater lake 30 km long by 1.5 km wide with an abyssal depth of more than 200 m. Based on previous temperature structure studies of this lake by Simpson and Woods (1970), at this time of the year (September 1970) there is a surface mixed layer of about 30 m at a temperature of  $\sim 12^{\circ}\text{C}$ , below which a thermocline rich in microstructure extends down to  $\sim 100$  m. At greater depths the temperature decreases only slightly to a value of  $5.3\text{--}5.7^{\circ}\text{C}$  at the bottom. An example of the raw data record collected by PROTAS is shown in Figure 10.45. Note that the two components of relative velocity  $u'$  and  $v'$  vary little in the surface layer down to 30 m. On reaching the thermocline, however, they exhibit marked fluctuations of up to  $\pm 1$  cm/s that are clearly associated with the temperature gradient. Below the thermocline, the shear diminishes, with relative velocities of  $<1$  mm/s in the deep water. The corrected profiles of the velocity shear components and density gradient, computed based on the profiles of the measured data digitized at intervals of 0.5 s, revealed (Simpson, 1972) a marked relation between the two

gradients, with the strongest shear closely coinciding with the region of largest temperature gradient. The shear exhibited a maximum value of  $1.6 \times 10^{-2}/\text{s}$ , which was found to be typical for all the records analyzed and of the same order as that observed by Woods (1969b). Results from sea trials that were undertaken in the stratified area of the western Irish Sea indicated the viability of PROTAS for observation of small-scale velocity shear in the ocean (Simpson, 1972).

#### 10.4.3. Free-Falling Lift-Force Sensitive Probes

It has been seen that the vane used in the free-fall instrument PROTAS (which profiles the horizontal velocity fluctuations by sensing the motion of a neutrally buoyant vane) reported by Simpson (1972) responds to changes in the horizontal velocity in a vertical distance approximately equal to 30 cm, i.e., the vertical resolution achievable by PROTAS is on the order of 30 cm. However, dye studies of Woods and Fosberry (1967) indicate that the shear is concentrated into regions on the order of 10 cm thick. Osborn (1974) reported an instrument that is capable of completely resolving a vertical profile of the vertical shear. The advantage of this high-resolution probe is that from the variance of the vertical shear, one can estimate the turbulent energy dissipation.

The velocity sensor described by Osborn (1974) is an adaptation of the two-component airfoil probe (Siddon, 1965, 1971a, b) to the oceanic environment (see Figure 10.46). The probe tip is an axisymmetric solid of revolution aligned with the major axis of the freely falling body. Variations  $u'$  in the horizontal velocity represent a fluctuating angle of attack of the total velocity vector, thereby causing a fluctuating lift force on the probe tip. Embedded in the probe tip are two piezoceramic bimorph beams from a ceramic phonograph cartridge that sense the components of the lift force into two perpendicular directions. To reduce the effect of the lead wires, two preamplifiers, one for each velocity component, are situated directly behind the probe in a small pressure case.

The oceanic measurements require an adaptation of Siddon's probe that has greater sensitivity and can operate at pressures on the order of 20 atm (= 200-m seawater depth). The probe, as far back as the preamplifier, is filled with epoxy. The epoxy tip is molded in place from the same epoxy, thereby waterproofing all the electrical contacts. Osborn and colleagues have routinely operated the probe to a depth of 230 m with no leakage. Tests they conducted in a pressure chamber showed that the probe is insensitive to changes in ambient pressure, even sudden changes on the order of 2 atm. Sufficient sensitivity was achieved by using a urethane-based epoxy with a hardness specification of 45

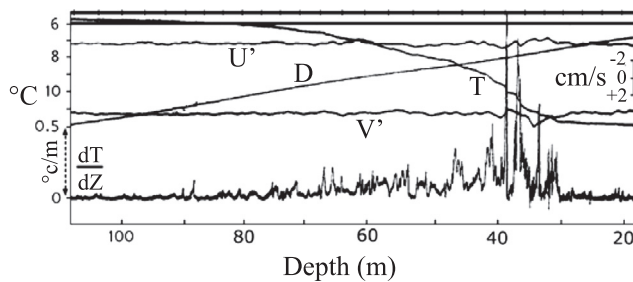


**FIGURE 10.45** Example of data record collected by PROTAS profiler probe from the Loch Ness freshwater lake. All parameters are recorded against time, which is indicated by marks at intervals of 10 s at the upper edge of the record. An equivalent depth scale is given at the lower edge. The meanings of symbols are as follows: D = depth; T = temperature;  $\frac{dT}{dz}$  = temperature gradient.  $u'$  and  $v'$  are the relative velocity components. Fall speed in this example is 33.3 cm/s. (Source: Simpson, 1972.)

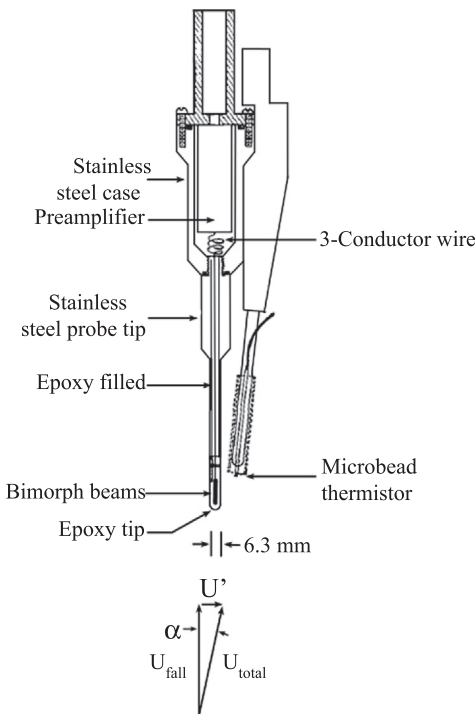


**FIGURE 10.46** Diagram of Osborn's velocity and temperature microstructure profiler probes. Vectors show that a change in the horizontal velocity relative to the probe tip appears as a change in the angle of attack of the overall velocity vector. (Source: Osborn, 1974, ©American Meteorological Society. Reprinted with permission.)

on the Shore A scale. An identical tip molded from an epoxy with Shore A hardness of 70 is 60 percent less sensitive. Unfortunately, because most urethane-based epoxies deteriorate in water, the probes have a lifetime in water on the order of 10 hours. However, accelerating technological advancement shows promise of superior-quality epoxies that are insensitive to water. The beams are mounted in a jig while being epoxied to the support and wire leads in order to make the channels orthogonal and to increase the reproducibility of the manufacturing process.

Because the probe is responding to the lift force, the probe's output voltage is proportional to the angle of attack and the mean velocity squared, i.e.,

$$V \approx S \left( \frac{1}{2} \rho \bar{u}^2 \right) \sin\alpha, \quad (10.12)$$

In this expression,  $V$  is the output voltage of the preamplifier,  $S$  is a calibration constant,  $\bar{u}$  is the mean velocity along the central axis of the probe, and  $\sin\alpha$  can be approximated by  $u'/u$ , where  $u'$  is the fluctuating horizontal velocity. Calibration of the probe gave a value of  $S$  as  $4 \times 10^{-3} \text{ V cm sec}^2 \text{ gm}^{-1}$ , with an estimated error of  $\pm 15$  percent. The resolution is equivalent to 0.1 cm/s at a fall speed of 25 cm/s.

The piezoceramic beams are inherently AC devices. The signals from the preamplifiers are sent to the glass

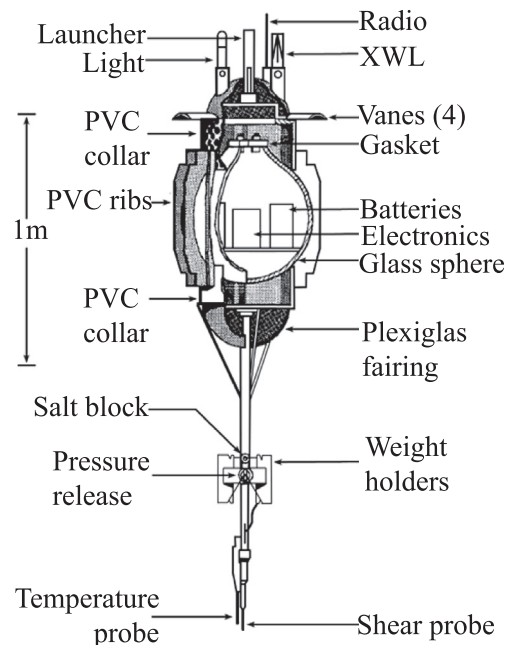


**FIGURE 10.47** Schematic diagram of Osborn's velocity and temperature microstructure profiler. (Source: Osborn, 1974, ©American Meteorological Society, reprinted with permission.)

sphere of the profiling instrument (see Figure 10.47) where, due to low-frequency drift in the preamplifiers, there is another low-frequency filter (3-db point at  $5 \times 10^{-2} \text{ Hz}$ ) before the final amplification. The response above 30 Hz is believed to be uniform to beyond 100 Hz, because the resonant frequency of the tip of the probe is between 1 and 2 kHz. The resonance is well damped.

Seawater temperature is sensed with a Veco 43A401C micro-bead thermistor, which is glass-coated and has a nominal diameter of 0.013 cm. It is mounted 2 cm from the velocity probe, and the maximum exposure to the flow is achieved by suspending the bead from its 0.0018-cm-diameter wire leads that extend on opposite sides of the bead.

The probe's fall speed is determined from a record of water pressure versus time sensed with a 0–500 psia Vibrotron pressure transducer mounted inside the glass sphere of the profiling instrument. Typical values of the fall speed are in the range 20–25 cm/s.

The body of the profiler rotates as it descends through the water column. Experience had shown that this rotation must be very slow, at a period of about  $\sim 20$  second per revolution, for the flow velocity data to be interpretable. With the short wings used, the lift force is small, and therefore the profiler is adjusted to be only slightly heavier (500 gm) than that of the displaced water. Another necessity for rotation of the profiler is determination of the orientation of the velocity sensors. Rotation is monitored as a function of time with a 3,000-turn coil wrapped around

a permeable iron core. With this technique, the coil produces a sinusoidal voltage as the body of the profiler rotates through Earth's magnetic field. The orientation of the coil relative to the bimorph beams of the probe is determined in the laboratory.

The two velocity signals, ambient seawater temperature, and its time derivative are converted from voltages to frequency-modulated (FM) signals using voltage-controlled oscillators operating on four standard IRIG frequencies. The Vibrotron pressure transducer is inherently an FM device operating on a standard IRIG channel. The five FM signals are multiplexed together and transmitted from the profiler to its support vessel along a Sippican Expendable Wire Length, which is essentially a Sippican Expendable Bathymeter without a thermistor or nose weight. It consists of two spools of very fine two-conductor wire (39 gauge), one spool being attached to the instrument and the other remaining on the support vessel. The wire is free spooling, i.e., it comes off the spool like a line off a spinning reel, and causes essentially no drag on the instrument as it falls through the water. In the frequency range used, there is large capacitive coupling between the two conductors, and therefore seawater is used as the signal return path.

The rotation rate of the profiler is telemetered directly up the wire as a slow variation on the offset voltage of the wire. An operational amplifier on the surface ship presents a high impedance load on the wire. The FM signals are recorded directly following high-pass filtering, and the rotation rate is recorded following low-pass filtering. The instrument descends until the weights are released by a Richardson-type stretched-pin release or by the dissolving of a salt block that acts as a back-up release. Upon return to the surface, the instrument is located with the aid of the flashing light and radio transmitter. An STD profile is taken immediately after each successful drop.

Figure 10.48 shows the data for an 8-m-thick region. The fall speed was  $20.7 \pm 0.5$  cm/s and the rotation period  $26 \pm 0.3$  s. There is a turbulent region 5 m thick wherein both the velocity traces and the temperature gradient show intense activity. Some activity is seen in the water above and below. According to Osborn, these data show a very complicated situation, the understanding of which would require information about the horizontal extent of the turbulent region. Figure 10.49 shows the spectrum of data from velocity channel 1 in Figure 10.48 taken at a fall speed of 20.7 cm/s. Temporal frequency times the spectral density of velocity is plotted against the logarithm of the temporal frequency. The plot is variance-preserving in the sense that the areas under the curve are proportional to the variance. Frequency times the spectral density of the vertical current shear, which is frequency-squared times the velocity spectrum, is also plotted. The rise in the shear spectrum above 14 Hz is due to noise.

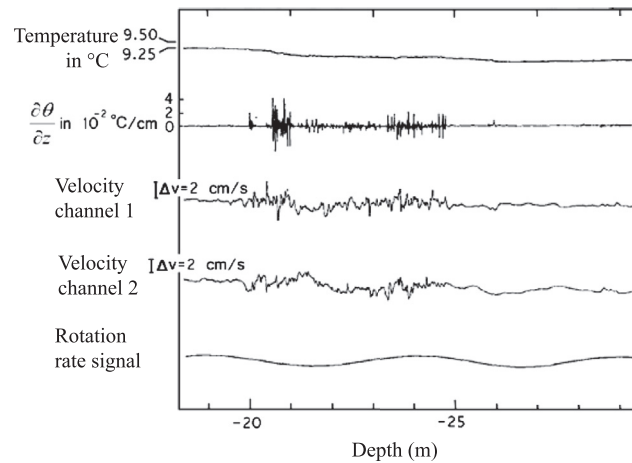


**FIGURE 10.48** Data collected by Osborn's velocity and temperature microstructure profiler on August 2, 1972, from Howe Sound. (Source: Osborn, 1974, ©American Meteorological Society, reprinted with permission.)

The velocity data are subject to low-frequency contamination due to pendulum-like oscillations of the instrument body. Some of the energy in the frequency bands below 0.1 Hz is from body motions. However, the spectrum of the shear shows that this low-frequency energy does not contribute to the estimate of the variances of the vertical current shear.

High-frequency contamination of the velocity data can come from the acceleration sensitivity of the probe. Vibration of the probe tip places an inertial load on the bimorph beams that is proportional to the amplitude and frequency of the vibration and the mass of the epoxy tip. These high-frequency vibrations can contribute significantly to an estimate of the variance of the vertical shear. The velocity data are differentiated in the instrument, thus giving the velocity shear directly and reducing the noise level in the shear spectra at high frequencies.

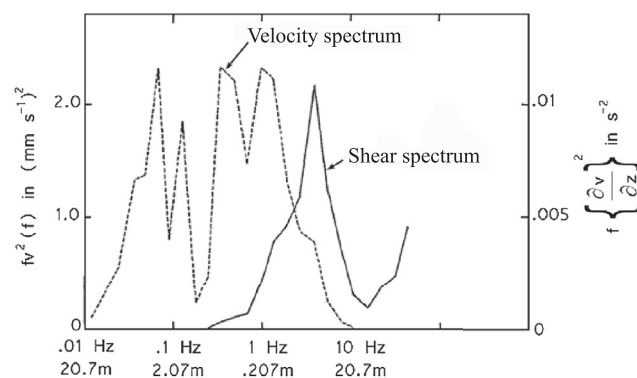


**FIGURE 10.49** Spectrum of data from velocity channel 1 shown in Figure 10.48, taken at a fall speed of 20.7 cm/s. The spectrum of the shear is frequency squared times the velocity spectrum. (Source: Osborn, 1974, ©American Meteorological Society, reprinted with permission.)

To ameliorate many of the difficulties found in the just-described probe, the instrument housing has been replaced by a long aluminum tube, similar to that of Simpson (1972), in order to (1) increase the stability of the free-fall body, (2) reduce oscillation of the body due to the eddies that are shed off the uppermost part of the housing, and (3) provide sufficient buoyancy. Osborn (1974) concludes that the airfoil probe combined with free-fall instrument housing is ideal for studying the vertical current shear in the ocean. According to him, the resolution and sensitivity are sufficient to provide estimates of the energy dissipation directly. In his measurements, the maximum value of the shear was 0.7/s, which is considerably larger than those reported by Simpson (1972) or Woods and Fosberry (1967).

## 10.5. MERITS AND LIMITATIONS OF FREELY SINKING/RISING UNGUIDED PROBES

It has been noted that freely sinking probes are an effective means for determining profiles of horizontal current velocity in the ocean. In comparison to a moored instrument, the freely sinking probe has been found to have certain advantages in that an entire profile is obtained from a single record and the measurements are not contaminated by mooring-line motions. However, there are difficulties in interpreting current-velocity profiles derived from freely sinking/rising probes, because the vehicle is affected by the flow it is attempting to measure.

Two basic techniques have been used to measure current profiles. In one method, the probe is acoustically tracked while it sinks or rises, much as a weather balloon is tracked by electromagnetic means. This method has been found to be effective in measuring the slowly varying component of the profile or relatively low wave-number variability. The assumption usually made is that the probe instantaneously follows the horizontal current; but high shears, where the horizontal current velocity changes abruptly, will result in high wave-number variability that the vehicle cannot follow.

In the second type of freely sinking/rising current-measuring probe, there is a current-velocity sensor that measures the current flow relative to the vehicle. Relative velocities are dominated by high wave-number variations because the vehicle will tend to follow low wave-number variations in the current-velocity profile, leaving only the higher wave-number variations in the measured relative-velocity profile. In other words, high-frequency velocity fluctuations are well represented in measurements from a velocity sensor on a freely sinking/rising vehicle, but lower frequencies become increasingly attenuated below the characteristic frequency of order  $1/\tau$ , where  $\tau$  is the time scale for the vehicle response.

Hendricks and Rodenbusch (1981) analyzed this problem and concluded that to increase the frequency resolution, it is necessary to minimize  $\tau$  by decreasing the mass or by increasing the sink/rise rate. According to them, the last option is probably the easiest technically, but the improvement in frequency resolution will not yield proportional gains in vertical wave number. Small vehicles are most effective as tracked current profilers to obtain maximum bandwidth in vertical wave number, whereas larger bodies will give greater wave-number resolution for vehicles measuring relative horizontal velocity with a velocimeter. In most cases, the velocity measurements are ultimately interpreted as a profile or vertical wave-number spectrum rather than a time series or frequency spectrum.

Another effect that may become significant for instruments of the second kind arises when the current-velocity sensors are offset from the main body of the vehicle. In many applications, the current-velocity sensor is not located near the vehicle's center of mass but is placed some distance above or below the main body. Often a placement is chosen to minimize hydrodynamic flow distortion at the sensor. Although it is desirable to minimize such distortion, offsetting the flow sensor introduces an artifact that must be accounted for in the interpretation of the velocity measurements. For example, when the sensors are located below the main body of a sinking vehicle, they measure the relative horizontal velocity before it is felt by the vehicle and before the vehicle can respond to the changes in the drag force. As a result, the sensed velocity difference will, generally, be greater than that which would be measured had the sensors been at the center of mass and the vehicle had accelerated in response to the velocity difference. When the flow sensor is offset as just mentioned, the sensors measure the velocity of a layer that is different from the one occupied by the bulk of the vehicle, thereby introducing a phase shift between the measured velocity and the vehicle velocity.

A third effect arises when the drag force on the body is distributed over a vertical length that is not short compared to the vertical length scales of the measured velocity variation. In this case, the actual drag force distribution must be accounted for to properly interpret the ocean-current velocity measurements.

## REFERENCES

- Berger, F.B., 1957. The nature of Doppler velocity measurement. IRE Transactions on Aeronautical and Navigational Electronics, ANE-4. September, 3, 103–112.
- Cole, D., 1981. A new glass deep-sea acoustically tracked current profiler. Proc. Oceans '81 Conference 1, 257–260.
- Cooper, J.W., Stommel, H., 1968. Regularly spaced steps in the main thermocline near Bermuda. J. Geophys. Res. 73, 5849–5854.
- Crease, J., 1962. Velocity measurements in the deep water of the Western North Atlantic. J. Geophys. Res. 67, 3173–3176.

- Drever, R.G., Sanford, T.B., 1970. A free fall electromagnetic current meter instrumentation. *Proc. I.E.R.E. Conf. on Electronic Engineering in Ocean Technology*. Swansea, 19, 353–370.
- Duda, T.F., Cox, C.S., 1987. Vorticity measurement in a region of coastal ocean eddies by observation of near-inertial oscillations. *Geophys. Res. Lett.* 14, 793–796.
- Duda, T.F., Cox, C.S., Deaton, T.K., 1988. The Cartesian diver: A self-profiling Lagrangian velocity recorder. *J. Atmos. Oceanic Technol.* 5, 16–33.
- Duing, W., Johnson, D., 1972. High resolution current profiling in the Straits of Florida. *Deep-Sea Res.* 19, 259–274.
- Evans, D.L., Rossby, H.T., Mork, M., Gytre, T., 1979. YVETTE: A free-fall shear profiler. *Deep-Sea Res.* 26/6A, 703–718.
- Evans, R., Leaman, K., 1978. A comparison between the Duing profiling current meter and the White Horse acoustic profiler. *J. Geophys. Res.* 83, 5515–5520.
- Garcia-Berdeal, I., Hautala, S.L., Thomas, L.N., Johnson, H.P., 2006. Vertical structure of time-dependent currents in a mid-ocean ridge axial valley. *Deep-Sea Res. I* 53, 367–386.
- Gould, W.J., Schmitz Jr., W.J., Wunsch, C., 1974. Preliminary field results for a Mid-Ocean Dynamics Experiment (MODE-O). *Deep-Sea Res.* 21, 911–931.
- Grant, H.L., Hughes, B.A., Vogeland, W.M., Molliet, A., 1968. The spectrum of temperature fluctuations in turbulent flow. *J. Fluid Mech.* 34, 423–442.
- Gregg, M.C., Cox, C.S., 1971. Measurements of the oceanic microstructure of temperature and electrical conductivity. *Deep-Sea Res.* 18, 925–934.
- Gregg, M.C., Cox, C.S., 1972. The vertical microstructure of temperature and salinity. *Deep-Sea Res.* 19, 355–376.
- Halkin, D., Rossby, T., 1985. The structure and transport of the Gulf Stream at 73°W. *J. Phys. Oceanogr.* 15, 1439–1452.
- Hamblin, P.F., Kuehnle, R., 1980. An evaluation of an unattended current and temperature profiler for deep lakes. *Limnol. Oceanogr.* 25, 1128–1141.
- Hayes, S.P., Milburn, H.B., Ford, E.F., 1984. TOPS: A free-fall velocity and CTD profiler. *J. Atmos. Oceanic Technol.* 1, 220–236.
- Hayward, G.G., Ferris, S.P., 1979. A new acoustic command system for recovery of oceanographic instruments. *Marine Technology Society Proceedings*, 139–144.
- Hendricks, P.J., Rodenbusch, G., 1981. Interpretation of velocity profiles measured by freely sinking probes. *Deep-Sea Research* 28A (10), 1199–1213.
- Hinze, J.O., 1959. Turbulence. McGraw-Hill, New York, NY, USA.
- Hogg, N.G., 1976. On spatially growing waves in the ocean. *J. Fluid. Mech.* 78, 217–235.
- Hoyt, J.K., 1982. The design of syntactic foam pressure housings for expendable acoustic beacons, one facet of a prototype current profiling instrument. M.S. thesis. Massachusetts Institute of Technology, Cambridge, MA, USA.
- Joseph, A., 2000. Applications of Doppler Effect in navigation and oceanography, Encyclopedia of Microcomputers, 25. Marcel Dekker, Newyork, USA, 17–45.
- Leaman, K.D., 1976. Observations on the vertical polarization and energy flux of near-inertial waves. *J. Phys. Oceanogr.* 6, 894–908.
- Leaman, K.D., Sanford, T.B., 1975. Vertical energy propagation of inertial waves: A vector spectral analysis of velocity profiles. *J. Geophys. Res.* 80, 1975–1978.
- Leaman, K.D., Sanford, T.B., 1975. Vertical energy propagation of inertial waves: a vector spectral analysis of velocity profiles. *J. Geophys. Res.* 80, 1975–1978.
- Leaman, K.D., Molinari, R.L., Vertes, P.S., 1987. Structure and variability of the Florida Current at 27°N: April 1982–July 1984. *J. Phys. Oceanogr.* 17, 565–583.
- Longuet-Higgins, M.S., Stern, M.E., Stommel, H., 1954. The electric field induced by ocean currents and waves, with applications to the method of towed electrodes. In: *Papers in Physical Oceanography and Meteorology*, 13. Woods Hole Oceanographic Institution and the Massachusetts Institute of Technology, Woods Hole, MA, USA, 1–37.
- Luyten, J.R., Swallow, J.C., 1976. Equatorial undercurrents. *Deep-Sea Res.* 23, 999–1000.
- Luyten, J.R., Swallow, J.C., 1976. Equatorial undercurrents. *Deep-Sea Res.* 23, 999–1001.
- Luyten, J.R., Needell, G., Thomson, J., 1982. An acoustic dropsonde: Design, performance, and evaluation. *Deep-Sea Res.* 29 (4A), 499–524.
- Mangelsdorf Jr., P.C., 1962. The world's longest salt bridge. In: *Marine Sciences Instrumentation*, Vol. 1. Plenum Press, Newyork, 173–185.
- Mullineaux, L.S., France, S.C., 1995. Dispersal mechanisms of deep-sea hydrothermal vent fauna. In: Humphris, S.E., Zierenberg, R.A., Mullineaux, L.S., Thomson, R.E. (Eds.), *Seafloor hydrothermal systems: Physical, chemical, Biological, and geological interactions*. American Geophysical Union, Washington, DC, USA, pp. 408–424.
- Nasmyth, P.W., 1970. Oceanic turbulence. Ph.D. dissertation. University of British Columbia, BC, Canada.
- Neshyba, S., Neil, V., Denner, W., 1971. Temperature and conductivity measurements under Ice Island T-3. *J. Geophys. Res.* 74, 8107–8119.
- Osborn, T.R., 1969. Oceanic fine structure. thesis. University of California, San Diego, CA, USA.
- Osborn, T.R., 1974. Vertical profiling of velocity microstructure. *J. Phys. Oceanogr.* 4, 109–115.
- Osborn, T.R., Cox, C.S., 1972. Oceanic fine structure. *Geophys. Fluid Dyn.* 3, 321–345.
- Perkins, H., 1970. Inertial oscillations in the Mediterranean. Ph.D. thesis. Massachusetts Institute of Technology and Woods Hole Oceanographic Institution.
- Plaisted, R.O., Richardson, W.S., 1970. Current fine structure in the Florida Current. *J. Mar. Res.* 28 (3), 359–363.
- Pochapsky, T.E., 1966. Measurements of deep water movements with instrumented neutrally buoyant floats. *J. Geophys. Res.* 71, 2491–2504.
- Pochapsky, T.E., Malone, F.D., 1972. A vertical profile of deep horizontal current near Cape Lookout, North Carolina. *J. Marine Res.* 30, 163–167.
- Price, J.F., Weller, R.A., Pinkel, R., 1986. Diurnal cycling: Observations and models of the upper ocean response to diurnal heating, cooling, and mixing. *J. Geophys. Res.* 91, 8411–8427.
- Richardson, W.S., Carr, A.R., White, H.J., 1969. Description of a freely dropped instrument for measuring current velocity. *J. Mar. Res.* 27, 153–157.
- Richardson, W.S., Schmitz Jr., W.J., 1965. A technique for the direct measurement of transport with application to the Straits of Florida. *J. Mar. Res.* 23, 172–185.
- Richardson, W.S., Schmitz Jr., W.J., 1965. A technique for the direct measurement of transport with application to the Straits of Florida. *J. Marine Res.* 16, 172–185.

- Riggs, N.P., 1989. Current profilers: Comparing three different techniques. *Sea Technology*, March issue, 52–54.
- Rona, P., Trivett, A., 1992. Discrete and diffuse heat transfer at ASHES vent field Axial Volcano, Juan de Fuca Ridge. *Earth Planetary Science Letters* 109, 57–71.
- Rossby, H.T., 1974. Studies of the vertical structure of horizontal currents near Bermuda. *J. Geophys. Res.* 79, 1781–1791.
- Rossby, H.T., Sanford, T.B., 1976. A study of velocity profiles through the main thermocline. *J. Phys. Oceanogr.* 6, 766–774.
- Rossby, H.T., Sanford, T.B., 1976. A study of velocity profiles through the main thermocline. *J. Phys. Oceanogr.* 6, 766–774.
- Rossby, T., 1969. A vertical profile of currents near Plantagenet Bank. *Deep-Sea Research* 16, 377–385.
- Royer, L., Hamblin, P.F., Boyce, F.M., 1986. Analysis of continuous vertical profiles in Lake Erie. *Atmosphere-Ocean* 21, 73–89.
- Royer, L., Hamblin, P.F., Boyce, F.M., 1987. A comparison of drogues, current meters, winds, and a vertical profiler in Lake Erie. *J. Great Lakes Res.* 13 (4), 578–586.
- Sanford, T.B., 1971. Motionally induced electric and magnetic fields in the sea. *J. Geophys. Res.* 76, 3476–3492.
- Sanford, T.B., 1975. Observations of the vertical structure of internal waves. *J. Geophys. Res.* 80, 3861–3871.
- Sanford, T.B., Drever, R.G., Dunlap, J.H., 1978. A velocity profiler based on the principles of geomagnetic induction. *Deep-Sea Research* 25, 183–210.
- Sanford, T.B., Drever, R.G., Dunlap, J.H., 1985. An acoustic Doppler and electromagnetic velocity profiler. *J. Atmos. Oceanic Technol.* 2 (2), 110–124.
- Sanford, T.B., Drever, R.G., Dunlap, J.H., D'Asaro, E.A., 1982. Design, operation, and performance of an expendable temperature and velocity profiler (XTVP). APL-UW 8110. Tech. Rep., Appl Phys Lab, University of Washington, Seattle, 88.
- Siddon, T.E., 1965. A turbulence probe using aerodynamic lift, Tech. Note 88, Institute for Aerospace Studies, University of Toronto, Toronto, Canada.
- Siddon, T.E., 1971a. A miniature turbulence gauge utilizing aerodynamic life. *Rev. Sci. Instr.* 42, 653–656.
- Siddon, T.E., 1971b. A new type of turbulence gauge for use in liquids. preprint of paper presented at Symposium on Flow, Inst. Soc. Amer., Pittsburgh, PA, USA.
- Simpson, J.H., 1972. A free-fall probe for the measurement of velocity microstructure. *Deep-Sea Res.* 19, 331–336.
- Simpson, J.H., Woods, J.D., 1970. The temperature microstructure in a freshwater thermocline. *Nature* 226 (5248), 832–834.
- Spain, P.F., Dorson, D.L., Rossby, H.T., 1981. Pegasus: A simple, acoustically tracked velocity profiler. *Deep-Sea Res.* 28A (12), 1553–1567.
- Stommel, H., Federov, K., 1967. Small-scale structure in temperature and salinity near Timor and Mindanao. *Tellus* 19, 306–325.
- Thomas, R.S., 1971. Measurement of ocean current shear using acoustic backscattering from the volume. *Deep-Sea Res.* 18, 141–143.
- Thomson, R.E., Gordon, R.L., Dymond, J., 1989. Acoustic Doppler current profiler observations of a mid-ocean ridge hydrothermal plume. *J. Geophys. Res.* 94, 4709–4720.
- Trivett, D.A., Williams, A.J., 1994. Effluent from diffuse hydrothermal venting. 2. Measurements of plumes from diffuse hydrothermal vents at the southern Juan de Fuca Ridge. *J. Geophys. Res.* 99, 18,417–18,432.
- Van Leer, J.C., Duing, W., Erath, R., Kennelly, E., Speidel, A., 1974. The cyclesonde: An unattended vertical profiler for scalar and vector quantities in the upper ocean. *Deep-Sea Res.* 21, 385–400.
- Voorhis, A.D., Bradley, A.M., 1984. Popup: A prototype bottom-moored long-term current profiler. *J. Atmos. Oceanic Technol.* 1, 166–175.
- Ward-Whate, P.M., 1977. A vertical automatic profiling system. Proc. MTS-IEEE Oceans '77 Conf. Record, 25B1–25B5.
- Webster, F., 1968. Observations of inertial-period motions in the deep sea. *Rev. Geophys.* 6, 473–490.
- Webster, F., 1969. On the representativeness of direct deep-sea current measurements. *Prog. Oceanogr.* 5, 3–15.
- Woods, J., 1968. CAT under water. *Weather* 23, 224–235.
- Woods, J.D., 1969a. On designing a probe to measure ocean microstructure. *Underwater Sci. Technol.* J. 1 (1), 6–12.
- Woods, J.D., 1969b. On Richardson's number as a criterion for laminar-turbulent-laminar transition in the ocean and atmosphere. *Radio Sci.* 4 (12), 1289–1298.
- Woods, J.D., Fosberry, G.G., 1967. The structure of the thermocline. Report 1966–1967, Underwater Association, London, 5–18.

## BIBLIOGRAPHY

- Miles, J.W., Howard, L.N., 1964. Notes on a heterogeneous shear flow. *J. Fluid Mech.* 20 (2), 331–336.
- Osborn, T.R., Cox, C.S., 1972. Oceanic fine structure. *Geophys. Fluid Dyn.* 3, 321–345.
- Pollard, R.T., Millard Jr., R.C., 1970. Comparison between observed and simulated wind-generated inertial oscillations. *Deep-Sea Res.* 17, 795–812.
- Rooth, C., Duing, W., 1971. On the detection of “inertial” waves with pycnocline followers. *J. Phys. Oceanogr.* 1, 12–16.
- Sanford, T.B., 1986. Recent improvements in ocean current measurement from motional electric fields and currents. Proc. IEEE Third Working Conference on Current Measurement, 22–24 January 1986. In: Airlie, Virginia, G., Appell, F., Woodward, W.E. (Eds.). Institute of Electrical & Electronic Engineers, New York, NY, USA, pp. 65–77.
- Schott, F., Lee, T.N., Zantop, R., 1988. Variability of structure and transport of the Florida Current in the period range of days to seasonal. *J. Phys. Oceanogr.* 18, 1209–1230.
- Takematsu, M., Kawatake, K., Koterayama, W., Suhara, T., Mitsuyasu, H., 1986. Moored instrument observations in the Kuroshio south of Kyushu. *J. Oceanographical Soc. Japan* 42, 201–211.
- Trump, C.L., Okawa, B.S., Hill, R.H., 1985. The characterization of a midocean front with a Doppler shear profiler and a thermistor chain. *Journal of Atmospheric and Oceanic Technology* 2, 508–516.
- Webster, F., 1968. Observations of inertial-period motions in the deep sea. *Rev. Geophys.* 6, 473–492.
- Webster, F., 1969. On the representativeness of direct deep-sea current measurements. *Prog. Oceanogr.* 5, 3–15.